

# **Flow Properties of Selected Pharmaceutical Powders**

A Thesis Submitted to the College of Graduate Studies and Research  
in partial fulfilment of the requirements for the degree of  
Master of Science  
in the Department of Chemical Engineering  
University of Saskatchewan

By  
Erica Emery

Copyright Erica Emery September 2008  
All Rights Reserved

## **Permission for Use**

The author has agreed that the Libraries of the University of Saskatchewan may make this thesis freely available for inspection. Moreover, the author has agreed that permission for extensive copying of this thesis for scholarly purposes may be granted by the professor(s) who supervised the thesis work recorded herein or, in their absence, by the Head of the Department of Chemical Engineering or the Dean of the College of Graduate Studies. Copying or publication or any other use of the thesis or parts thereof for financial gain without written approval by the University of Saskatchewan is prohibited. It is also understood that due recognition will be given to the author of this thesis and to the University of Saskatchewan in any use of the material of the thesis.

Request for permission to copy or to make other use of material in this thesis in whole or in part should be addressed to:

Head  
Department of Chemical Engineering  
University of Saskatchewan  
57 Campus Drive  
Saskatoon, Saskatchewan  
S7N 5A9  
Canada

## **Abstract**

In the pharmaceutical industry uniform flow of powders is one of the most important considerations in solid dosage manufacture [3, 7, 8]. Improper feeding of powders from storage hoppers into dye-presses can lead to inconsistent product quality, causing economic and health impacts. Investigation into the properties affecting powder flow is crucial.

There were four objectives of the current research:

1. To determine the effect of moisture on the flow (Jenike flow index, Hausner Ratio and Carr Index, static and dynamic angle of repose) of selected pharmaceutical powders.
2. To study the effect of particle shape and size on Jenike flow index for selected starch and pharmaceutical powders.
3. To determine the effect of mixture compositions on the Jenike flow index of ordered mixtures of selected pharmaceutical powders.
4. To develop a novel flowability tester based on electrical capacitance tomography (ECT) that measures the dynamic angle of repose of powders.

To address the first objective, to determine the effect of moisture content on the flow of four pharmaceutical powders; an active pharmaceutical ingredient (API), aspartame, hydroxypropyl methylcellulose (HPMC), and Respitose® ML001 were selected. The API and Respitose® powders were found to be nonhygroscopic and were tested at near zero moisture contents only (in this case 0.31% and 0.19% respectively). Aspartame was tested at moisture contents of 0%, 2%, 5% and 8% and HPMC at moisture contents of 0%, 2%, 5% and 10%. Powder flowability was measured using the Jenike shear index,

the Hausner Ratio, the Carr Index and the static and dynamic angles of repose. The Jenike flow index of aspartame increased from 0.885 to 3.65 with an increase in moisture content, which was attributed to the formation of large, round agglomerates. The Jenike flow index of HPMC decreased from 3.28 to 2.65 with an increase in moisture content, which was attributed to the increasing strength of liquid bridges. The Jenike flow index was the only flowability indicator to capture this complex behaviour.

In order to address the second objective, five starches (cow cockle, barley, rye, rice and tapioca), as well as four pharmaceutical ingredients (an API, aspartame, HPMC, and Respitose® ML001), were characterised for size and shape, and then tested for flowability. Powder flowability was measured using the Jenike shear test, the most widely accepted flowability standard in the pharmaceutical industry. It was found that the Jenike flow index decreased linearly with decreasing aspect ratio and decreasing roundness for the powders investigated. It was also determined that particle shape had a greater impact on flowability than size for powders under 30 µm in diameter.

To address the third objective, ordered mixtures of pharmaceutical powders were examined to determine their flowability. Six combinations of Respitose® ML001, hydroxypropyl methylcellulose (HPMC), and an active pharmaceutical ingredient (API) in varying concentrations were selected for investigation. Powder flowability was measured using the Jenike shear test, the most widely accepted flowability standard in the industry. The Jenike flow indices of the ordered mixtures were indistinguishable from the Jenike flow index of pure Respitose® at the  $\alpha = 0.1$  level.

The fourth objective, to develop a novel flowability tester using electrical capacitance tomography to measure the dynamic angle of repose, was investigated at the same time as the effect of moisture content. It was determined that the results of the novel dynamic angle of repose tester did not correlate well with the Jenike shear test. More development is needed before the novel flowability tester is ready for industrial use. The Jenike shear cell remains the only acceptable flow test for complex flow behaviour.

## **Acknowledgement**

My sincere thanks to Dr. Pugsley and Dr. Sharma, my co-supervisors. Your advice and especially helpful proof-reading were essential in the completion of this manuscript. Thank you to my committee members, Dr. Tyler and Dr. Evitts, for your comments and encouragement.

I also would like to thank Mr. R. Blondin, Mr. T. Wallentiny, and Mr. D. Claude of the Department of Chemical Engineering and Mr. A. Kozlow of the Department of Civil Engineering for their technical assistance at various stages of this work. Recognition is also due to Mr. H. Berg and all the members of the Engineering Shops. Finally, thank you to the members of the fluidization and particle characterization group for your support.

Financial assistance from Eli Lilly and the Department of Chemical Engineering is gratefully acknowledged.

## Table of Contents

Permission for Use.....	i
Abstract .....	ii
Acknowledgement .....	v
Table of Contents.....	vi
List of Figures .....	ix
List of Tables .....	x
List of Symbols .....	x
Chapter 1. Introduction .....	1
1. Background .....	1
1.1 Powder Properties Affecting Flow.....	2
1.2 Knowledge Gap .....	3
1.3 Research Objectives.....	4
1.4 Thesis Format.....	5
1.5 References .....	5
Chapter 2. Introduction to Moist Powders .....	8
2.1 Contribution of this Paper to the Overall Study.....	8
2.2 Contribution of the Master's Candidate.....	8
2.3 Factors affecting Powder Flow .....	9
2.4 Effects of Moisture on Powder Flow .....	9
2.5 Measures of Powder Flowability .....	10
2.6 Additional Experimental Details.....	13
2.7 References .....	15
Chapter 3. Flowability of Moist Pharmaceutical Powders .....	18
3.1 Abstract: .....	18
3.2 Introduction.....	18
3.2.1 Importance of Powder flow .....	18
3.2.2 Effect of Moisture .....	19
3.2.3 Knowledge Gap .....	20
3.2.4 Research Objectives.....	21

3.3 Materials and Methods.....	21
3.3.1 Powders Used.....	21
3.3.2 Moisture Sorption Isotherms.....	22
3.3.3 Hausner Ratio and Carr Index.....	25
3.3.4 Static Angle of Repose.....	26
3.3.5 Dynamic Angle of Repose .....	26
3.3.6 Shear Tests .....	27
3.4 Results.....	28
3.4.1 Hausner Ratio and Carr Index.....	28
3.4.2 Static Angle of Repose.....	30
3.4.3 Dynamic Angle of Repose .....	32
3.4.4 Shear Tests .....	33
3.4.5 Comparison of Flow Tests: .....	36
3.5 Conclusions.....	37
3.6 Acknowledgement .....	37
3.7 References.....	37
Chapter 4. Introduction to the Effect of Size and Shape on Powder Flowability.....	41
4.1 Contribution of this Paper to the Overall Study.....	41
4.2 Contribution of the Master's Candidate.....	41
4.3 Background on Starches .....	42
4.4 Background on Pharmaceutical Powders.....	42
4.5 References.....	44
Chapter 5. Influence of Shape and Size on Flowability of Pharmaceutical Powders.....	45
5.1 Abstract .....	45
5.2 Introduction.....	45
5.2.1 Size Effects .....	46
5.2.2 Shape Effects .....	47
5.2.3 Knowledge Gap .....	47
5.3 Materials and Methods.....	48
5.3.1 Powders Selected .....	48
5.3.2 Particle Characterization.....	49



5.3.3 Shear Tests: .....	51
5.4 Results .....	52
5.4.1 Particle Characterization .....	52
5.4.2 Shear Test Results .....	56
5.5 Conclusions .....	62
5.6 Nomenclature .....	63
5.7 References .....	63
Chapter 6. Introduction to the Effect of Mixture Composition .....	66
6.1 Contribution of this Paper to the Overall Study .....	66
6.2 Contribution of the Master's Candidate .....	66
6.3 Background on Ordered Mixtures .....	66
6.4 Additional Experimental Details .....	67
6.5 References .....	68
Chapter 7. Flowability of Ordered Mixtures .....	69
7.1 Abstract .....	69
7.2 Introduction .....	69
7.2.1 Glidants .....	70
7.2.2 Ordered Mixtures .....	70
7.2.3 Knowledge Gap .....	72
7.3 Materials and Methods .....	72
7.3.1 Mixtures Selected .....	72
7.3.2 Powder Flow Tests .....	73
7.3.3 Inversina Mixer .....	74
7.4 Results .....	74
7.5 Conclusions .....	77
7.6 Recommendations .....	78
Chapter 8. Conclusions and Recommendations .....	81
8.1 Effect of Moisture Content .....	81
8.2 Effect of Particle Shape and Size .....	82
8.3 Effect of Fines Content (Ordered Mixtures) .....	82
8.4 Comparison of Flow Tests (Novel Dynamic Angle of Repose Tester) .....	83

Appendix A: Compressibility Test Results.....	85
Appendix B: Static Angle of Repose Test Results .....	87
Appendix C: Dynamic Angle of Repose Test Results.....	89
Appendix D: Jenike Shear Test Results.....	91
Appendix E: Skeletal Density of Powders.....	95

## List of Figures

Figure 1.1: Powder Flow Regimes and Common Problems.....	2
Figure 2.1: ECT Dynamic Angle of Repose Flowability Tester.....	14
Figure 2.2: Output of the ECT Dynamic Angle of Repose Test.....	15
Figure 3.1: Equilibrium Moisture Sorption Isotherms of the Test Pharmaceutical Powders.....	23
Figure 3.2: Humidity Control System.....	24
Figure 3.3: Hausner Ratio of Moist Pharmaceutical Powders.....	29
Figure 3.4: Carr Index of Moist Pharmaceutical Powders.....	30
Figure 3.5: Static Angle of Repose of Moist Pharmaceutical Powders.....	31
Figure 3.6: Dynamic Angle of Repose of Nonhygroscopic Pharmaceutical Powders.....	32
Figure 3.7: Dynamic Angle of Repose of Moist Pharmaceutical Powders.....	33
Figure 3.8: Representative Graph of Shear Results.....	34
Figures 3.9: Flow Index of Aspartame.....	35
Figure 3.10: Flow Index of HPMC.....	36
Figure 4.1: Chemical formula of Pharmaceutical Powders (a) Aspartame, b) HPMC, c) Lactose Monohydrate).....	43

Figure 5.1: Scanning Electron Microscope Images of Selected Starch Powders.....	53
Figure 5.2: Microscope and SEM images of Pharmaceutical Powders.....	54
Figure 5.3: Jenike Flow Function of Selected Starch Powders.....	56
Figure 5.4: Jenike Flow Function of Selected Pharmaceutical Powders (a) Aspartame, b) API, c) HPMC, d) Respitose® ML001).....	57
Figure 5.5: Effect of Size and Shape on Jenike Flow Index of Selected Powders (a) ECD, b) Aspect Ratio, c) Roundness, d) Irregularity).....	61
Figure 6.1: Test of the Inversina Mixer (50% power for 5minutes).....	66
Figure 7.1: Jenike Flow Index of Ordered Mixtures.....	74
Figure 7.2: Effect of Fines Content on Jenike Flow Index of Ordered Mixtures.....	76

## List of Tables

Table 2.1: Jenike classification of powder flowability by flow index ( $ff_c$ ).....	12
Table 5.1: Jenike classification of powder flowability by flow index ( $ff_c$ ).....	51
Table 5.2: Shape factors for selected starches.....	54
Table 5.3: Shape factors for selected pharmaceutical powders.....	55
Table 7.1: Dry powder composition of ordered mixtures.....	72

## List of Symbols

$A$	area ( $\mu\text{m}^2$ )
$BD$	bulk density ( $\text{g}/\text{cm}^3$ )
$b$	minor axis ( $\mu\text{m}$ )
$CI$	Carr Index (%)
$F_C$	unconfined yield strength (kPa)
$ff_c$	Jenike flow index
$HR$	Hausner Ratio

$l$	major axis ( $\mu\text{m}$ )
$P$	perimeter ( $\mu\text{m}$ )
$TD$	tapped density ( $\text{g}/\text{cm}^3$ )
$\sigma_I$	major consolidating stress (kPa)

# **Chapter 1**

## **Introduction**

### **1. Background**

Powders are ubiquitous; they can be found in almost every industry. Good flowability of the powders is important in each of these industries. Although there is no single definition for “good flowability”, it is generally taken to mean that the powder flows reliably without assistance [1]. Blending, transfer, storage, feeding, compaction, and fluidization all depend on good powder flowability [2, 3]. Designing and troubleshooting mass flow hoppers requires the measurement of powder flow [4, 5]. Tableting operations require excipients with the desired flow, physical and mechanical properties [6]. In the pharmaceutical industry in particular, uniform flow of solid mixtures is one of the most important considerations in solid dosage manufacture [3, 7, 8].

Powders can discharge from hoppers or storage bins in one of two flow regimes: mass flow or funnel flow. In mass flow, which is the desirable hopper flow regime, all of the powder in the hopper is in motion [2, 5]. This regime is also referred to as “first-in-first-out” flow since the powder that enters the hopper first and resides at the hopper base is also the first to exit the hopper when it is opened. In funnel or core flow, the central core of powder exits the bin or hopper first, followed by the remaining powder from the sides of the container. This regime is also referred to as “first-in-last-out” flow since material that has entered the hopper first and resides at the sides of the hopper will remain there until all other material above it has drained through the core or collapsed from the walls

above. If the material along the edges of the bin remains in place and doesn't exit the container, a "rathole" forms [3-5, 9]. These concepts are illustrated in Figure 1.1.

Occasionally a stable dome or arch will form across the bottom of the bin or hopper, preventing any discharge. The formation of this stagnant mass of material is known as "arching" [5, 10]. When the dome of material is disturbed, uncontrolled flow of powder, or "flooding" can occur [3, 11]. Powder mixtures containing material of different size and density are also known to segregate or de-mix when disturbed [3, 5, 6, 12].

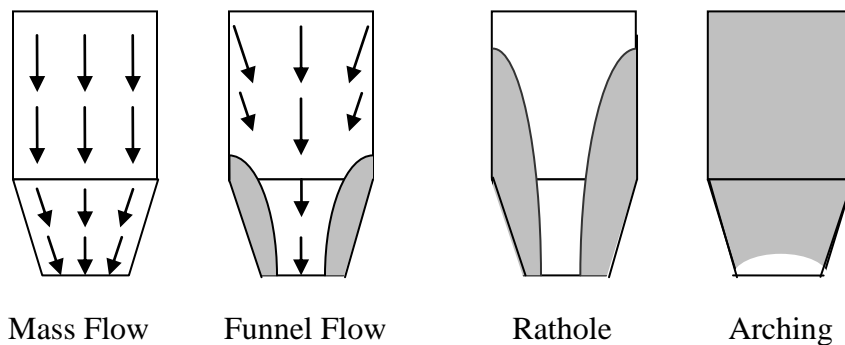


***Figure 1.1: Powder Flow Regimes and Common Problems***

## **1.1 Powder Properties Affecting Flow**

Some powders are free-flowing and easily enter the mass flow regime, while others are cohesive and, therefore, do not flow as readily. Powder flow is governed more by physical than by chemical properties [7]. The flow properties of powders are known to depend on the size, shape and size distribution of particles [1, 2, 13-16], as well as moisture content and time-consolidation [17-20]. Small, irregularly-shaped powders are generally considered to cause more flow difficulties than large, well-rounded ones [5].

However, Fitzpatrick et al. [5] found no significant relationship between powder properties and their flowability, which illustrates the complexity of powder flow and the likely interaction between these physical properties. In the case of particle diameters less than approximately ten microns, inter-particle cohesive forces reach the same order of magnitude as the gravitational force [4, 20]. Cohesive forces can include mechanical forces arising from the meshing or interlocking of surface asperities and irregularities, solid bridges formed from recrystallization, capillary forces in an adsorbed liquid layer, Van der Waals forces, and electrostatic forces [16, 18, 21, 22]. These cohesive forces are not present in all powders, and their relative effect may vary from one powder to another [5].

## **1.2 Knowledge Gap**

There is limited information in the open literature as to the effect of moisture on the flowability of pharmaceutical powders. There have been several studies on food powders, coal and various other powders, but few on pharmaceutical binders, excipients, active pharmaceutical ingredients (API) and other additives. It is unclear what the effects of moisture on these powders will be.

There is also a need for a better understanding of which powder properties affect flowability the most. Ideal powders for such a study are starches, which occur naturally in a variety of shapes and sizes.

The effect of fines content, i.e. the composition of ordered mixtures, is another area that is not well understood. To date there have been several papers published on the flowability of ordered mixtures and the effect of glidants. However, none have used an actual amorphous crystalline needle-shaped API as the glidant particle.

Finally, there is no single flow tester that has been universally accepted as both reliable and easy-to-use for the determination of powder flowability. Jenike shear tests, which represent the industry standard, are difficult to operate and time consuming. On the other hand, there is controversy over the accuracy of other “simple” testers used to determine flowability.

### **1.3 Research Objectives**

The selected gaps in the knowledge described above led to the following four objectives of the current research:

1. To determine the effect of moisture on the Jenike flow index, Hausner Ratio, Carr Index and static and dynamic angle of repose of selected pharmaceutical powders.
2. To determine the effect of particle shape (aspect ratio, roundness, irregularity) and size (equivalent circle diameter) on the Jenike flow index of selected starch and pharmaceutical powders.
3. To determine the effect of mixture composition of six ordered mixtures of API, Respitose® and HPMC on the Jenike flow index.
4. To develop a novel flowability tester based on electrical capacitance tomography (ECT) that measures the dynamic angle of repose of powders.



## 1.4 Thesis Format

This thesis is written in article-based format, with every second chapter corresponding to a paper that has been submitted to a peer-reviewed journal. Transition “chapters” between each article are used to tie the work together, present additional information that may not be present in the article but that is relevant for this thesis, and to outline the contributions of each of the authors. Finally, a concluding chapter is added to summarize the work.

## 1.5 References

- [1] B.H. Kaye. Characterizing the flowability of a powder using the concepts of fractal geometry and chaos theory, *Particle & Particle System Characterisation*. 14 (1997) 53-66.
- [2] A. Faqih, A. Alexander, F. Muzzio, M.S. Tomassone. A method for predicting hopper flow characteristics of pharmaceutical powders, *Chemical Engineering Science*. 62 (2007) 1536-1542.
- [3] J. Prescott, R. Barnum. On powder flowability, *Pharmaceutical Technology*. 24 (2000) 60-84.
- [4] T.A. Bell. Industrial needs in solids flow for the 21<sup>st</sup> century, *Powder Handling and Processing*. 11 (1999) 9-12.
- [5] J. Fitzpatrick, S.A. Barringer, T. Iqbal. Flow property measurements of food powders and sensitivity of Jenike’s hopper design methodology to the measured values, *Journal of Food Engineering*. 61 (2004) 399-405.
- [6] M. Mullarney, B. Hancock, G. Carlson, D. Ladipo, B. Langdon. The powder flow and compact mechanical properties of sucrose and three high-intensity sweeteners used in chewable tablets, *International Journal of Pharmaceuticals*. 257 (2003) 227-236.
- [7] K. Thalberg, D. Lindholm, A. Axelsson. Comparison of different flowability tests for powders for inhalation, *Powder Technology*. 146 (2006) 206-213.

- [8] R. Hedge, J.L. Rheingold, S. Welch, C.T. Rhodes. Studies of powder flow using a recording powder flowmeter and measurement of the dynamic angle of repose, *Journal of Pharmaceutical Sciences*. 74 (1985) 11-15.
- [9] J.M. Hill, G.M. Cox. Rat-hole stress profiles for shear-index granular materials, *Acta Mechanica*. 155 (2002) 157-172.
- [10] A. Drescher, A.J. Waters, C.A. Rhoades. Arching in hoppers: I. Arching theories and bulk material flow properties, *Powder Technology*. 84 (1995) 165-176.
- [11] D. Geldart, J.C. Williams. Flooding from hoppers: Identifying powders likely to give problems, *Powder Technology*. 43 (1985) 181-183.
- [12] C. Dury, G. Ristow. Boundary effects on the angle of repose in rotating cylinders, *The American Physical Society*. 57 (1998) 4491-4497.
- [13] M.M. Von Eisenhart-Rothe, I.A.S.Z. Peschl. Powder testing techniques for solving industrial problems, *Chemical Engineering*. 84 (1977) 97-103.
- [14] T.E. Durney, T.P. Meloy. Particle shape effects due to crushing method and size, *International Journal of Mineral Processing*. 16 (1986) 109-123.
- [15] S. Kamath, V.M. Puri, H.B. Manbeck. Flow property measurement using the Jenike cell for wheat flour at various moisture contents and consolidation times, *Powder Technology*. 81 (1994) 293-297.
- [16] I.A.S.Z. Peschl, F. Sigulinski. Flowability tests of powders, *Powder Metallurgy International*. 22 (1990) 31-34.
- [17] M. Rhodes, *Introduction to Particle Technology*, John Wiley & Sons, Toronto, 1998.
- [18] H. Abou-Chakra, U. Tüzün. Microstructural blending of coal to enhance flowability, *Powder Technology*. 111 (2000) 200-209.
- [19] A. Bodhimage, Correlation between physical properties and flowability indicators for fine powders, (2006).
- [20] A. Castellanos, J. Valverde, A. Perez, A. Ramos, P.K. Watson. Flow regimes in fine cohesive powders, *The American Physical Society*. 82 (1999) 1156-1159.

[21] J. Cain. An alternative technique for determining ANSI/CEMA Standard 550 flowability ratings for granular materials, Powder Handling and Processing. 14 (2002) 218-220.

[22] M.E. Plinke, D. Leitch, F. Loffler. Cohesion in granular materials, Bulk Solids Handling. 14 (1994) 101-106.

## **Chapter 2**

### **Introduction to Moist Powders**

The following chapter (3.0) was submitted for publication to Powder Technology and is currently undergoing peer review. This transition chapter provides some additional background for the thesis that was not included in the manuscript, where it was assumed that the reader had a certain level of technical familiarity with the field.

#### **Citation**

E Emery, J Oliver, T Pugsley, J Sharma, J Zhou. The flowability of moist pharmaceutical powders, Powder Technology. submitted (2008). [1]

### **2.1 Contribution of this Paper to the Overall Study**

In this paper the effect of moisture on the flow of selected pharmaceutical powders (API, aspartame, HPMC, Respitose® ML001) is investigated, addressing objective #1. Also, the relative ranking of a series of flowability tests is compared. Specifically, the novel flowability tester based on electrical capacitance tomography (ECT) to measure the dynamic angle of repose of powders is compared to the industry standard Jenike shear test. This addresses objective #4 of the thesis.

### **2.2 Contribution of the Master's Candidate**

Experiments were planned by Erica Emery and Todd Pugsley, and performed by Erica Emery and Jasmine Oliver (an undergraduate student who worked in the lab during the summer of 2007). Todd Pugsley and Jitendra Sharma were consulted for advice on

experimental procedures. All writing was done by Erica Emery, with editorial advice from Todd Pugsley, Jitendra Sharma and Joe Zhou (Eli Lilly, the industrial partner in this work).

### **2.3 Factors affecting Powder Flow**

Some powders are free-flowing and easily enter the mass flow regime, while others are cohesive and, therefore, do not flow as readily. The flow properties of particulate solids are known to depend on the size, shape and size distribution of particles [2], as well as moisture content and time-consolidation [3-6]. Small, irregularly-shaped particles cause more flow difficulties than large, well-rounded ones [6, 7]. However, Fitzpatrick et al. [7] found no significant relationship between physical particle properties and their flowability. In the case of particle diameters less than approximately ten microns, gravitational forces are dominated by inter-particle cohesive forces for pharmaceutical and food powders[5, 8]. Cohesive forces can include mechanical forces arising from the meshing or interlocking of surface asperities and irregularities, solid bridges formed from recrystallization, capillary forces in an adsorbed liquid layer, Van der Waals forces, and electrostatic forces [4, 9]. These cohesive forces are not present in all powders, and their relative effect may vary from one powder to another [7].

### **2.4 Effects of Moisture on Powder Flow**

In general, increasing the moisture content of a powder decreases its ability to flow smoothly [7, 9]. The main reason for this is the increased thickness of the adsorbed

liquid layer, which increases the strength of liquid bridges formed between particles [7, 9].

Soluble powders stored for several days in an uncontrolled environment may be affected by caking due to moisture migration. At night, as the temperature outside the storage container drops, moisture migrates from the center of the powder mass towards the edges. If the moisture concentration becomes sufficiently high, liquid bridges form. When the temperature subsequently increases, the moisture evaporates or diffuses back to the center of the bulk, forming a solid bridge from the previously dissolved powder. This cycling repeats night after night, resulting in stronger bonds and formation of a cake [10-12].

## **2.5 Measures of Powder Flowability**

Powder flowability can be expressed in many different ways, using one or more of the myriad of measurement techniques available [14, 15]. The Jenike flow function and the corresponding flow index, which are based on the results of several direct shear tests, are the most widely accepted industry standards for the measurement of flowability [7, 8, 16-18].

Direct shear tests involve two important steps: pre-shear and shear. The powder is loaded into the shear cell and consolidated at a normal load that depends on the bulk density of the material. The powder is then sheared at this same normal load, which is referred to as the pre-shear load. The normal load is then reduced to a fraction of the pre-shear load and shearing begins. From a plot of shear stress at failure versus normal stress, it is

possible to calculate the powder properties of cohesion (y-intercept), the angle of internal friction (slope), and the yield locus [4, 16, 19]. There are two methods of constructing the instantaneous yield locus: the linear method [equation (2.1)] and the Warren-Spring method [equation (2.2)].

$$\sigma = \sigma_n \tan \phi + C \quad (2.1)$$

$$\left( \frac{\sigma_t}{C} \right)^n = \frac{\sigma_n}{\sigma_0} + 1 \quad (2.2)$$

In equations (2.1) and (2.2),  $\sigma$  is stress,  $\sigma_n$  is the normal stress,  $\phi$  is the angle of internal friction,  $C$  is cohesion,  $\sigma_t$  is the tensile yield stress and  $n$  is a constant in the range of 1-2 [7, 18]. According to Fitzpatrick et al. [7], the Warren-Spring equation is the preferred equation to describe the shape of a yield locus; however, Drescher et al. [18] found that the approximation used to construct the yield locus (linear or non-linear) had little effect on the shape of the Jenike flow function, as defined below. In light of this, the linear approximation was employed in the present study, as it is much simpler to implement.

From two Mohr's circles drawn tangent to the yield locus, the unconfined yield strength and major consolidating stress at each pre-shear load can be determined [7]. A plot of unconfined yield strength versus major consolidating stress is known as the Jenike flow function [7]. The flow index,  $ff_c$ , is the inverse of the slope of the flow function, and represents the strength of a consolidated powder that must be overcome before flow can occur [4, 7]. A steep slope of the flow function corresponds to a cohesive powder with poor or difficult flow; a flat slope corresponds to smooth powder flow [4]. Flow becomes more difficult as one moves in an anti-clockwise direction on the flow function plot [7].

A sample plot is provided in the following chapter (Figure 3.8). Table 2.1 presents rules-of-thumb that relate powder flowability to the flow index [7].

Table 2.1: Jenike classification of powder flowability by flow index ( $ff_c$ ) [7]

Flowability	Hardened	Very Cohesive	Cohesive	Easy Flow	Free Flow
Flow index	<1	<2	<4	<10	>10

The Jenike shear test technique has proven to be reproducible and valid for a wide range of powders [8]. However, shear testing is complicated and requires technical knowledge and hands-on skill [8]. It is also time-consuming, operator-dependent and potentially costly when high-value powder is tested and discarded [7, 8].

The Hausner Ratio and Carr Index are two additional flowability indicators that can be determined from bulk and tapped density tests. The Hausner Ratio is calculated from equation (2.3), where BD is the powder bulk density, and TD is the powder tapped density [17].

$$HR = \frac{TD}{BD} \quad (2.3)$$

Carr Index is calculated from equation (2.4) [17].

$$CI = \frac{TD - BD}{TD} \times 100\% \quad (2.4)$$

According to Cain et al. [17], the Hausner Ratio and Carr Index are comparable to the Jenike shear test in terms of predicting the relative flowability of powders. It is also



widely recognized that these tests are much easier to perform [17]. However, the Hausner Ratio may be sensitive to the apparatus used [14].

Another simple measure of flowability is the static angle of repose. The static angle of repose is the angle formed between the side of a stationary pile of powder and the horizontal [17]; the greater the angle of repose, the more cohesive the powder. ISO Standard 3435 uses angle of repose as a quantitative measure of cohesiveness of a granular material [17]. According to Bell [14], the static angle of repose is one of the best-known measures of flowability, but suffers from poor reproducibility. One of the main problems is that the angle formed by cohesive powders is not stable; it builds up to a steep angle then collapses to a much shallower one [9].

The dynamic angle of repose is a variation on the static angle of repose, where the angle is formed between powder in a rotating drum and the horizontal. Again, the greater the angle, the more cohesive the powder [20, 21]. At first, the powder builds up to a steep angle and collapses to a shallow one, but after several revolutions it steadies to a specific angle [20, 21]. This angle is dependent on the speed of rotation [20]. In traditional dynamic angle of repose tests, this angle is measured through the end-caps of a clear plastic drum which, according to Dury et al. [20], can lead to an error of 5% or more.

## **2.6 Additional Experimental Details**

Dynamic angle of repose depends on powder size, shape and mass, frictional forces between the powder and the drum wall, and the angular velocity of the rotating drum [5,

20, 22-24]. There are commercially available dynamic angle of repose testers that are simple to use and reportedly give reproducible results [25]. A novel dynamic angle of repose tester, using electrical capacitance tomography (ECT), was developed by our group at the University of Saskatchewan. Twelve sensors were arranged in a cylindrical configuration. A second cylinder, loaded half full of test powder, was inserted inside the sensor array. This secondary Teflon cylinder is rotated at speeds between 1 and 7 rpm. The ECT dynamic angle of repose tester is pictured in Figure 2.1.



***Figure 2.1: ECT Dynamic Angle of Repose Flowability Tester***

Capacitance measurements are recorded by a computer every  $1/10^{\text{th}}$  of a second. The difference in dielectric constants between air and the test powder inside the test cylinder allows the capacitance measurements to be reconstructed as tomographical information.

A Matlab<sup>TM</sup> computer program was used to reconstruct the data in a series of pictures like that given in Figure 2.2. More details on the operating principle of electrical capacitance tomography can be found in the work of Malcus et al. [26].

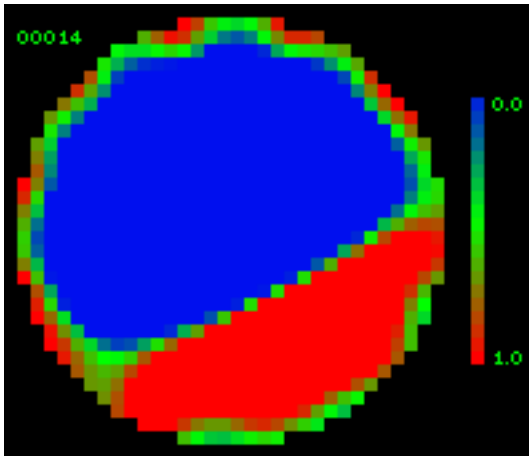


**Figure 2.2:** *Output of the ECT Dynamic Angle of Repose Test*

## 2.7 References

- [1] E. Emery, J. Oliver, T. Pugsley, J. Sharma, J. Zhou. The flowability of moist pharmaceutical powders, Powder Technology. submitted (2008).
- [2] T.E. Durney, T.P. Meloy. Particle shape effects due to crushing method and size, International Journal of Mineral Processing. 16 (1986) 109-123.
- [3] A. Bodhmag, Correlation between physical properties and flowability Indicators for fine powders, (2006).
- [4] H. Abou-Chakra, U. Tüzün. Microstructural blending of coal to enhance flowability, Powder Technology. 111 (2000) 200-209.
- [5] A. Castellanos, J. Valverde, A. Perez, A. Ramos, P.K. Watson. Flow regimes in fine cohesive powders, The America Physical Society. 82 (1999) 1156-1159.
- [6] M. Rhodes, Introduction to Particle Technology, John Wiley & Sons, Toronto, 1998.

- [7] J. Fitzpatrick, S.A. Barringer, T. Iqbal. Flow property measurements of food powders and sensitivity of Jenike's hopper design methodology to the measured values, *Journal of Food Engineering*. 61 (2004) 399-405.
- [8] T.A. Bell. Industrial needs in solids flow for the 21<sup>st</sup> century, *Powder Handling and Processing*. 11 (1999) 9-12.
- [9] M.E. Plinke, D. Leitch, F. Löffler. Cohesion in granular materials, *Bulk Solids Handling*. 14 (1994) 101-106.
- [10] G.I. Tardos. Ingress of atmospheric moisture into bulk powders: II. Application to caking of fine crystalline powders, *Powder Processing & Handling*. 8 (1996) 215-220.
- [11] E. Teunou, J.J. Fitzpatrick, E.C. Synnott. Characterisation of food powder flowability, *Journal of Food Engineering*. 39 (1999) 31-37.
- [12] T. Kollman, J. Tomas. Time consolidation and caking behaviour of soluble particulate solids, *Bulk Solids Handling*. 21 (2001) 431-434.
- [13] G.I. Tardos, I.V. Nicolaescu, B. Ahtchi-Ali. Ingress of atmospheric moisture into packed bulk powders, *Powder Processing & Handling*. 8 (1996) 7-15.
- [14] T.A. Bell, Flowability measurement and interpretation in industry, *Handbook of Conveying and Handling of Particulate Solids*, 10th ed., 2001, pp. 3-13.
- [15] J. Fitzpatrick, L. Ahrné. Food powder handling and processing: Industry problems, knowledge barriers and research opportunities, *Chemical Engineering and Processing*. 44 (2005) 209-214.
- [16] S. Kamath, V.M. Puri, H.B. Manbeck. Flow property measurement using the Jenike cell for wheat flour at various moisture contents and consolidation times, *Powder Technology*. 81 (1994) 293-297.
- [17] J. Cain. An alternative technique for determining ANSI/CEMA Standard 550 flowability ratings for granular materials, *Powder Handling and Processing*. 14 (2002) 218-220.
- [18] A. Drescher, A.J. Waters, C.A. Rhoades. Arching in hoppers: I. Arching theories and bulk material flow properties, *Powder Technology*. 84 (1995) 165-176.

- [19] K. Chang, D. Kim, S. Kim, M. Jung. Bulk flow properties of model food powder at different water activity, *International Journal of Food Properties*. 1 (1998) 45-55.
- [20] C. Dury, G. Ristow. Boundary effects on the angle of repose in rotating cylinders, *The American Physical Society*. 57 (1998) 4491-4497.
- [21] R. Hedge, J.L. Rheingold, S. Welch, C.T. Rhodes. Studies of powder flow using a recording powder flowmeter and measurement of the dynamic angle of repose, *Journal of Pharmaceutical Sciences*. 74 (1985) 11-15.
- [22] B.H. Kaye. Characterizing the flowability of a powder using the concepts of fractal geometry and chaos theory, *Particle & Particle System Characterisation*. 14 (1997) 53-66.
- [23] K.M. Hill, J. Kakalios. Reversible axial segregation of binary mixtures of granular material, *Physical Review E*. 49 (1994) R3610-R3613.
- [24] K. Yamane, T. Tanaka, Y. Tsuji, M. Nakagawa, S.A. Altobelli, DEM and MRI studies of particulate flows in a rotating cylinder". *Flow visualisation and image processing of multiphase systems, Flow Visualization and Image Processing of Multiphase Systems, FED (series) v.209 ed., ASME, 1995, pp. 225-228.*
- [25] J.L.P. Soh, C.V. Liew, P.W.S. Heng. New indices to characterize powder flow based on their avalanching behaviour, *Pharmaceutical development and technology*. 11 (2006) 93-102.
- [26] S. Malcus, G. Chaplin, T. Pugsley. The hydrodynamics of the high-density bottom zone in a CFB riser analyzed by means of electrical capacitance tomography (ECT), *Chemical Engineering Science*. 55 (2000) 4129-4138.

## **Chapter 3**

### **Flowability of Moist Pharmaceutical Powders**

Erica Emery, Jasmine Oliver, Todd Pugsley, and Jitendra Sharma, University of Saskatchewan; Joe Zhou, Eli Lilly

#### **3.1 Abstract:**

The effect of moisture content on four pharmaceutical powders (an active pharmaceutical ingredient (API), aspartame, hydroxypropyl methylcellulose (HPMC) and Respitose® ML001) was investigated. The API and Respitose® powders were found to be nonhygroscopic and were tested at their native moisture contents only. Aspartame was tested at moisture contents of 0%, 2%, 5% and 8% wet basis and HPMC at moisture contents of 0%, 2%, 5% and 10% wet basis. Powder flowability was measured using the Jenike shear index, the Hausner Ratio, the Carr Index and the static and dynamic angles of repose. The flowability of Aspartame increased with an increase in moisture content, which was attributed to the formation of large, round agglomerates. The flowability of HPMC decreased with an increase in moisture content, which was attributed to the increasing strength of liquid bridges. The Jenike shear index was the only flowability indicator to capture this complex behaviour.

#### **3.2 Introduction**

##### **3.2.1 Importance of Powder Flow**

It has been reported that approximately 75% of chemical manufacturing processes involve particulate solids at some stage [1]. Transport, storage and handling of

particulate solids are especially important in the pharmaceutical industry, where nearly 80% of products are in solid dosage form [2]. According to Dury et al. [3], the behaviour of granular materials has been researched for over 200 years. Despite this, accurate prediction of powder flow behaviour from a knowledge of particle size, shape or moisture content is still not possible [4].

### **3.2.2 Effect of Moisture**

In general, increasing the moisture content of a powder decreases its ability to flow smoothly [5, 6]. One of the main causes is the increased thickness of the adsorbed liquid layer, which increases the strength of liquid bridges formed between particles [5, 6]. For example, Abou-Chakra et al. [7] found that only the surface moisture of coal, and not its inherent or crystalline moisture, affected its flowability. Increased surface moisture caused increased surface tension, which caused cohesion between particles [7]. Amidon et al. [8] found the flow of microcrystalline cellulose decreased with an increase in moisture content, especially at moisture contents over 5%. Chang et al. [9] saw an increase in Hausner Ratio, angle of repose and shear stress (all of which indicate a decrease in flowability) as the moisture content of their food powders increased.

While the above-referenced studies found a decrease in powder flowability with increasing moisture content, this may not always be the case. According to Coelho et al. [10], Van der Waals forces are strengthened by adsorbed moisture because the added thickness of the moisture layer decreases interparticle distance by increasing the apparent diameter of the particle. Electrostatic forces, on the other hand, decrease with increasing

moisture content because of the conductive properties of water [10]. Friction and interlocking, which are caused by surface roughness, are decreased by moisture, which acts as a lubricant [10]. In another paper published by Coelho et al. [11], an improvement in mixture quality above a specific moisture content was noted when mixing ballotini and sand. The mixture quality was good for very dry conditions, then decreased with addition of water up to a point, beyond which mixture quality improved again [11].

Ibqual et al. [12] and Teunou et al. [13] both found an increase in cohesion, and a decrease in flowability, when the moisture content of several food powders was increased. Kamath et al. [14] found the angle of internal friction of wheat flour increased with an increase in moisture content. Nokhodchi et al. [15] found an increase in moisture content in hydroxypropyl methylcellulose (HPMC) lowered the glass transition temperature of the amorphous powder and increased the tensile strength of compacts formed from it.

### **3.2.3 Knowledge Gap**

Previous studies on the effect of moisture on powder flowability have reported differing trends. Also, there is limited information in the open literature as to the effect of moisture on the flowability of pharmaceutical powders. Furthermore, there is no flowability test that has been universally accepted as both reliable and easy to use. Jenike shear tests are difficult to conduct and time consuming, so an alternative test is desirable. However,



there is controversy over the accuracy of the other “simple” tests (Hausner Ratio, Carr Index, static and dynamic angle of repose) used to determine flowability.

### **3.2.4 Research Objectives**

The objectives of this research were: 1) to determine the effect of moisture content on the flowability of selected pharmaceutical powders, 2) to determine which flowability tests accurately describe the effect of moisture content on powder flowability.

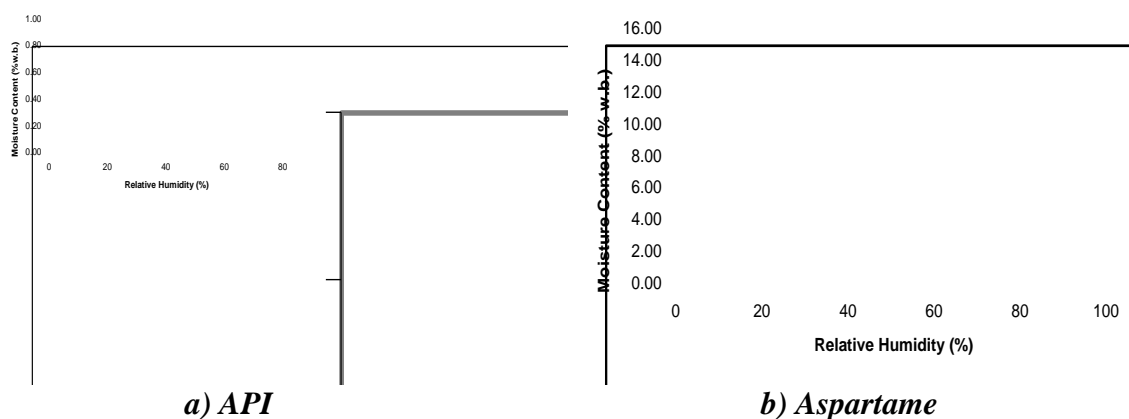
## **3.3 Materials and Methods**

### **3.3.1 Powders Used**

In this experiment, the flowability of an active pharmaceutical ingredient (API), aspartame, Respitose® ML001, and hydroxypropyl methylcellulose (HPMC) were determined. The particular API that was used had exhibited poor flowability in an industrial setting in the past. Aspartame is a commercially available sweetener that also tends to exhibit poor flow characteristics. Respitose® ML001 is a lactose monohydrate product commonly used as a pharmaceutical excipient. HPMC is a common pharmaceutical binding agent, as well as a retarding agent in solid dosage formulations [16]. These powders were chosen because they are widely used in industry and they span a range of particle shapes and sizes. In addition, it was anticipated that these powders would exhibit a range of moisture uptakes in humid air.

### 3.3.2 Moisture Sorption Isotherms

Powders exposed to the atmosphere can adsorb moisture from the air [17], and the amount they adsorb at a particular temperature is described by the equilibrium moisture sorption isotherm of the powder. The equilibrium moisture sorption isotherms of all four pharmaceutical powders were determined experimentally in the range of 8% to 76% relative humidity. This relative humidity range was chosen to cover the range of working conditions likely encountered in manufacturing plants. The relative humidity of ten containers was controlled using saturated salt solutions, as describe by Rowley and Mackin [18]. A 1-2 g powder sample was suspended in each container for a period of 24 hours at 20°C, to allow the powders to come to equilibrium. A halogen moisture analyzer (model HB43, Mettler Toledo, Columbus, OH), the measurement principle of which is based upon weight loss on drying, was used to determine the amount of moisture adsorbed at each relative humidity. The moisture analyser has an accuracy of  $\pm 0.30\%$ . The resulting isotherms shown in Figure 3.1 are an average of three trials.



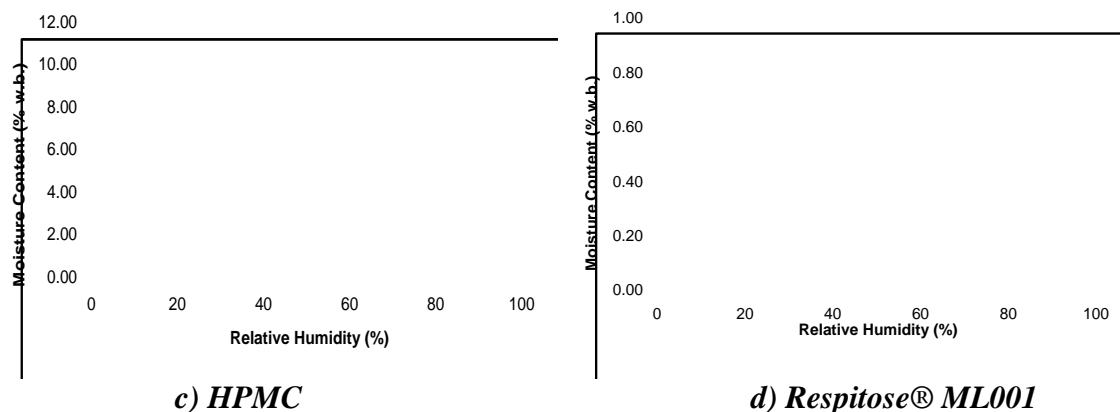


**Figure 3.1: Equilibrium Moisture Sorption Isotherms of the Test Pharmaceutical Powders**

Based on the above equilibrium moisture sorption isotherms, four moisture contents were chosen for aspartame and HPMC. The first was a nearly 0% moisture content obtained by drying the powders in an oven at 105°C for 24 hours prior to testing. Aspartame was also tested at approximately 2%, 5% and 8% moisture contents, while the HPMC was tested at approximately 0%, 2%, 5% and 10% moisture contents. The API and Respitose® ML001 powders appeared to be nonhygroscopic; i.e. their moisture content was independent of the surrounding environment. Hence, they were tested at only one moisture content. The moisture content reported for each test result is an average of the powder moisture content before and after the test.

Flowability tests required samples of each powder larger than could be humidified in the saturated salt solution containers. A humidity control system was designed based on the description of a similar apparatus by Stanford and DellaCorte [19]. In this apparatus, humidifying air is separated into two streams: the first passes through a gas diffusion

bubbler and the second is a bypass. The streams are then re-combined and sent to the humidity chamber containing the powder sample. A diagram of the system is presented in Figure 3.2. This system is controlled using two variable area flow meters on the air lines.

The cubic Plexiglas sample chamber is 30 cm on a side, with a plenum section at the bottom where air is introduced. Up to 900 cm<sup>3</sup> of powder can be supported on a porous tray made of 200-mesh stainless steel. The powder layer is 1-2 cm thick, which allows the moisture to equilibrate quickly throughout the bed. A humidity probe (model EE23, E+E Elektronik, Engerwitzdorf, Austria) was inserted 20 cm up the side of the chamber to measure the humidity of the air inside. The moisture content of the powders was measured with the same halogen moisture analyzer mentioned previously (model HB43, Mettler Toledo, Columbus, OH).

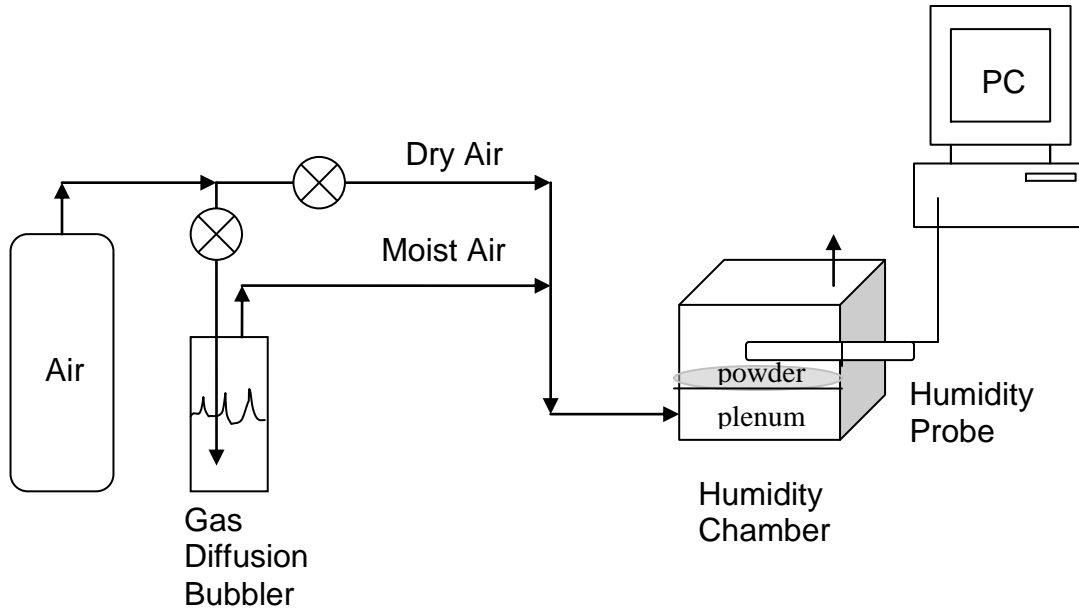


**Figure 3.2: Humidity Control System**

### 3.3.3 Hausner Ratio and Carr Index

The Hausner Ratio and Carr Index are both calculated from compressibility data [20]. The test powder is gently loaded through a funnel into a 100 ml cylinder and weighed to calculate its bulk density. Next, the cylinder is tapped in a single platform tapped density meter (Varian Canada Inc., Mississauga, ON), until the volume stops changing, in this case 1500 times. The Hausner Ratio is calculated from equation (3.1) and the Carr Index from equation (3.2), where BD is the powder bulk density and TD is the powder tapped density [21]. These tests were repeated three times for each moist powder.

$$HR = \frac{TD}{BD} \quad (3.1)$$

$$CI = \frac{TD - BD}{TD} \times 100\% \quad (3.2)$$

### **3.3.4 Static Angle of Repose**

The static angle of repose flowability test was performed following the procedure described by Bodhimage [2]. A conical funnel was mounted with its stem 6 cm from the horizontal surface. Between 50 and 100 grams of powder were poured through the funnel, enough that the top of the resulting pile reached the funnel outlet. Pictures were taken with a digital camera, and analyzed using a shareware image analysis program (Scion Image, [http://www.scioncorp.com/pages/scion\\_image\\_windows.htm](http://www.scioncorp.com/pages/scion_image_windows.htm)). The angle measured on the right and left hand sides of the pile were averaged to give a single static angle of repose. The greater the angle of repose, the more cohesive the powder [20]. This test was repeated three times for each moist powder.

### **3.3.5 Dynamic Angle of Repose**

A novel method using electrical capacitance tomography (ECT) to view the behaviour of the powder in the center of a rotating cylinder was used to determine the dynamic angle of repose. This eliminates the 5% or greater error due to end-cap effects as noted by Dury et al. [3]. A Teflon cylinder is loaded one third full and attached to the shaft of a low speed gear motor. Then the cylinder is rotated at 1 rpm, 3 rpm, and 7 rpm for a total of 100 seconds each. The location of the powder in the cylinder is recorded by the ECT computer every  $1/10^{\text{th}}$  of a second. A complete description of the measurement principle and image reconstruction method of the ECT is beyond the scope of this paper. For further information, the reader is referred to Malcus et al. [22]. The angle formed by the powder and the horizontal is measured from the resulting ECT images and plotted, with the final steady state angle reported as the dynamic angle of repose. As with the static

angle of repose, a higher angle corresponds to a more cohesive powder [3, 23]. This test was repeated twice for each moist powder.

### **3.3.6 Shear Tests**

The Jenike flow function and the corresponding flow index, which are based on the results of several direct shear tests, are the most widely accepted industry standards for the measurement of flowability [4, 5, 14, 20, 24]. The shear cell used in this study is a parallel plate direct shear cell, with a load cell calibrated for 0-100N. It consists of a 6 cm x 6 cm shear box, connected to a motor, the load cell, and a computer to record the output. The cross-sectional area of the shear cell before shear is  $3.546 \times 10^{-3} \text{ m}^2$ . It shears at a fixed rate of 48 mm/h. The cross-sectional area at any time is calculated from the width and the length remaining after subtracting the distance travelled from the length of the side of the shear box.

Three pre-shear loads were chosen based on ASTM Standard D 6128-00. The standard recommends pre-shear loads of 1.5 kPa, 3 kPa and 6 kPa for powders of low bulk density. Because of the selection of weights available the shear tests were actually performed with pre-shear normal loads of 1.601 kPa, 3.745 kPa, and 5.604 kPa. The standard also advises including the weight of the top half of the shear cell in the load calculation. Since the top half of the direct shear cell weighs over 2 kg, it was deemed unlikely the powder would support its weight, and it was not included in the normal load calculation. Tests with the shear box empty of powder, and with a sample of the wall material in the bottom half of the box confirmed that the stress measured is the powder-

to-powder shear, and not simply the shear strength of the equipment. A program was written in Matlab® ([www.mathworks.com](http://www.mathworks.com)) to assist with the analysis of the results. Three tests at each of the three pre-shear loads are necessary to construct the yield locus. This test was repeated twice for each moist powder.

From two Mohr's circles drawn tangent to the yield locus, the unconfined yield strength and major consolidating stress at each pre-shear load can be determined [5]. A plot of unconfined yield strength ( $F_c$ ) versus major consolidating stress ( $\sigma_1$ ) is known as the Jenike flow function [5]. The flow index,  $ff_c$ , is the inverse of the slope of the flow function and represents the strength of a consolidated powder that must be overcome before flow can occur [5, 7]. A steep slope of the flow function corresponds to a cohesive powder with poor or difficult flow; a flat slope corresponds to smooth powder flow [7]. Flow becomes more difficult as one moves in an anti-clockwise direction on the flow function plot [5].

### **3.4 Results**

#### **3.4.1 Hausner Ratio and Carr Index**

As they exhibited no difference in moisture content when exposed to air of differing relative humidities, the API and Respitose® ML001 were tested at a single moisture contents. At 0.12% wet basis moisture content, the API had a Hausner Ratio of 1.6 and a Carr Index of 39%. Both of these measurements are indicative of a cohesive powder [20]. Respitose® at 0.19% moisture content had an average Hausner Ratio of 1.7 and a Carr Index of 39%. These measurements also indicate a cohesive powder.



Both aspartame and HPMC were tested at four moisture contents. The resulting changes in Hausner Ratio and Carr Index with moisture content are shown in Figures 3.3 and 3.4. For Aspartame, a bi-linear increase in Hausner Ratio and Carr Index was observed with increasing moisture content, which indicates a decrease in flowability. The error bars shown in the figures represent one standard deviation from the mean. Based on the mean and standard deviation, Student's t-test was performed to test for statistically significant differences between the Carr Index and Hausner Ratio at each moisture content. Only the flowability at 0% moisture content was different from the flowabilities at other moisture contents at the  $\alpha = 0.1$  level of significance. The flowability of aspartame decreased significantly between 0% and 2% moisture, but then remained constant at the higher moisture contents tested. The increase in Hausner Ratio and Carr Index with increased moisture content is consistent with the study of Change et al. [9].

The Hausner Ratio and Carr Index of HPMC are independent of moisture content. There was no change in either the Hausner Ratio or the Carr Index at the  $\alpha = 0.1$  level of significance. Nokhodchi et al. [16] found that moisture content had a significant effect on the compressibility of HPMC. In reality, the flowability of both HPMC and aspartame may be changing, but it is not reflected in the Carr Index and Hausner Ratio. The Hausner Ratio and Carr Index are insensitive to changes in moisture content for the tapped density apparatus used here. This supports the claims of Soh et al. [25] that compressibility tests suffer from low differentiation and are sensitive to the apparatus

used. Abdullah et al. [26] also found the Hausner Ratio to be independent of moisture content.

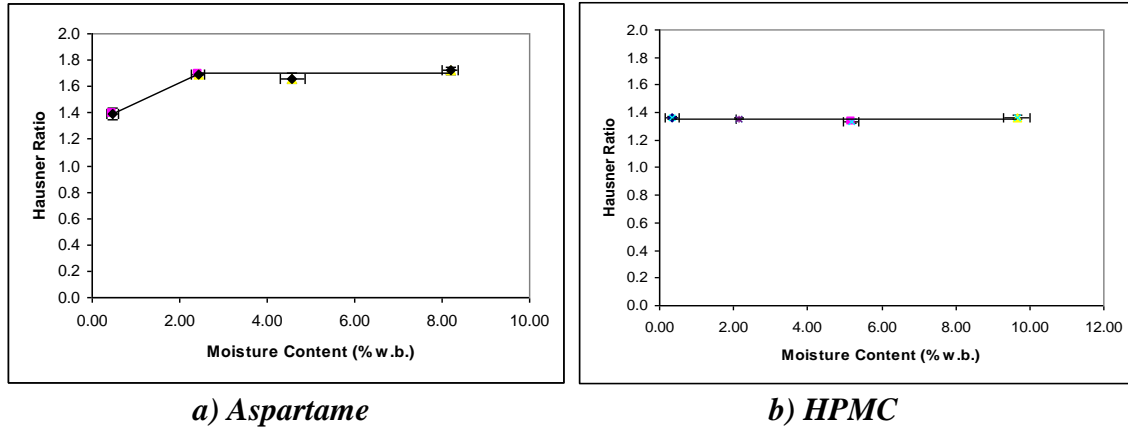


**Figure 3.3: Hausner Ratio of Moist Pharmaceutical Powders**

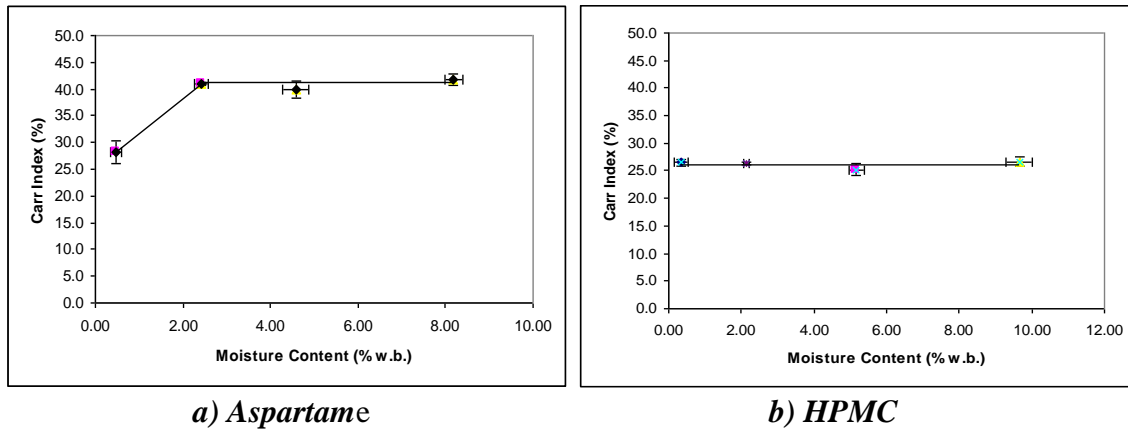


**Figure 3.4: Carr Index of Moist Pharmaceutical Powders**

### 3.4.2 Static Angle of Repose

API at a moisture content of 0.31% had an angle of repose of 47°, while Respitose® ML001 at 0.19% moisture content had an angle of repose of 52°. According to Cain

[20], a static angle of repose greater than  $40^\circ$  indicates a cohesive powder, whereas an angle greater than  $50^\circ$  indicates a very cohesive powder.

Aspartame again showed a bi-linear decrease in flowability with an increase in moisture content, as illustrated by the increase in angle of repose (Figure 3.5a). From 0% to 2% moisture, the change in angle was rapid; after this point, there was no statistically significant change at the  $\alpha = 0.1$  level. The HPMC data also showed a trend of increasing angle of repose, which is consistent with a decrease in flowability (Figure 3.5b). However, when Student's t-test was applied to the data from each of the four trials for each moisture content, it was found that there was no statistically significant difference between the angles of repose at any moisture content. Like the compressibility tests, the static angle of repose is also insensitive to the influence of moisture content on powder flowability.

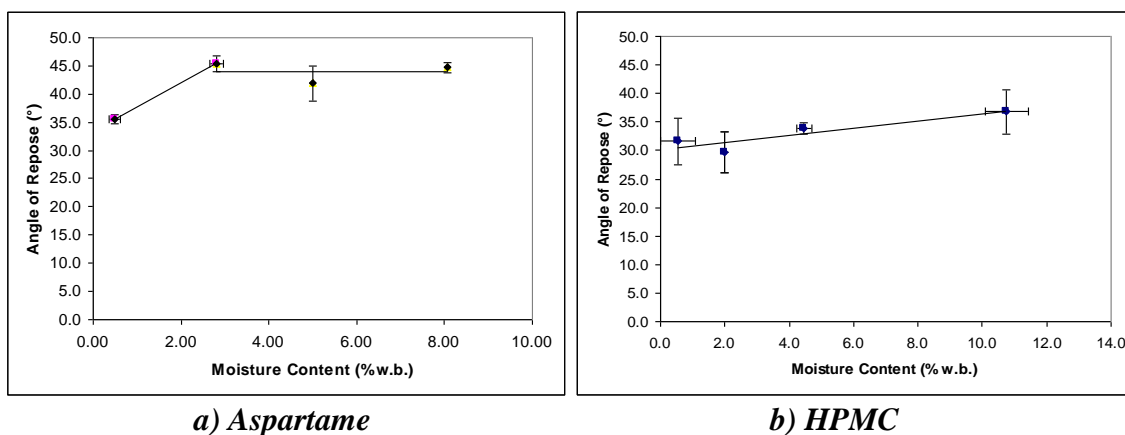


**Figure 3.5: Static Angle of Repose of Moist Pharmaceutical Powders**

### 3.4.3 Dynamic Angle of Repose

The API at a moisture content of 0.13% had an average dynamic angle of repose of  $44^\circ$  at 1 rpm, increasing to  $57^\circ$  at 7 rpm. Respitose® ML001 at 0.19% moisture content had an average dynamic angle of repose of  $39^\circ$  at 1 rpm, increasing to  $43^\circ$  at 7 rpm. Applying the same classification as was used for the static angle of repose to the dynamic angle of repose, both powders exhibited cohesive behaviour. The results are shown graphically in Figure 3.6. In both cases, the dynamic angle of repose increased linearly with an increase in rotational speed, as is generally reported in the existing literature [27-30]. However, application of Student's t-test to this data indicated that the increase was not statistically significant at the  $\alpha = 0.1$  level of significance.

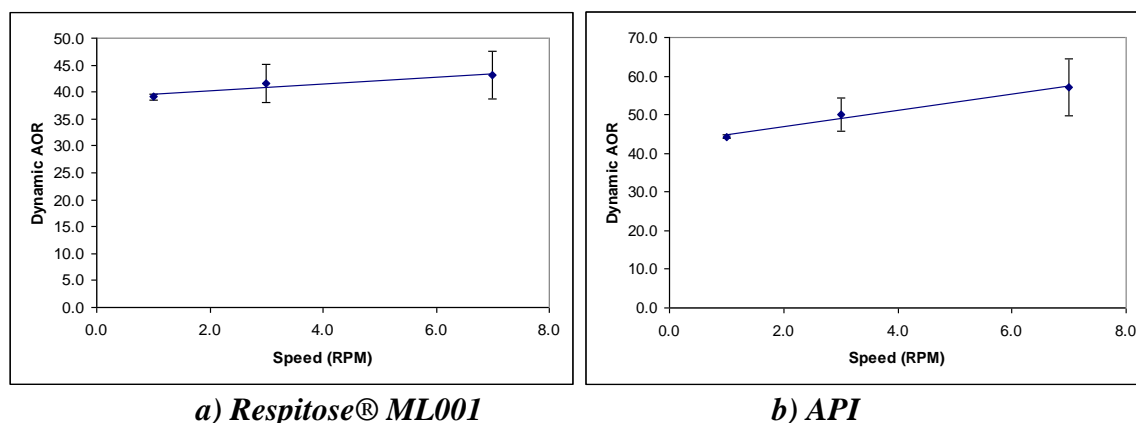


**Figure 3.6: Dynamic Angle of Repose of Nonhygroscopic Pharmaceutical Powders**

The dynamic angle of repose of the two moist powders (aspartame and HPMC) did not increase monotonically with increasing rotational speed as it did for Respitose® and the API. Instead, the flowability of aspartame first decreased (i.e. an increase in dynamic angle of repose), and then increased with a further increase in moisture content. The flowability of HPMC seemed to increase with increasing moisture content, as indicated

by a decrease in dynamic angle of repose. The data are plotted in Figure 3.7. The large variability in the results and the lack of a concrete relationship between moisture content and angle indicate that this novel dynamic angle of repose tester requires more study before it can enter widespread industrial use. At the moment, it appears that the technique suffers from the same level of insensitivity as the other methods described previously.

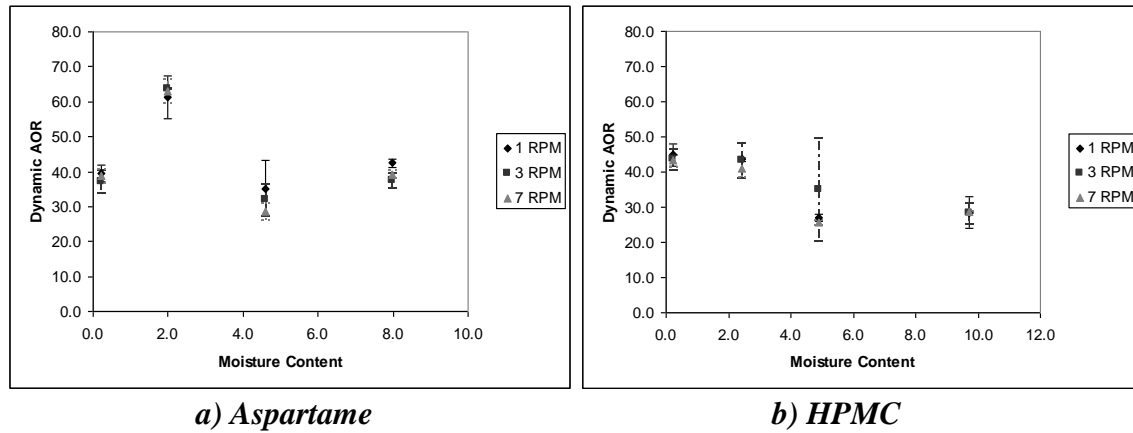


**Figure 3.7: Dynamic Angle of Repose of Moist Pharmaceutical Powders**

### 3.4.4 Shear Tests

The Matlab® program for analyzing shear cell results uses a least-squares analysis to find the best-fit line to describe the yield locus. The line is then interpolated to find the Mohr's circles tangent to the yield locus and to determine the unconfined yield strength ( $F_c$ ) and the major consolidation stress ( $\sigma_1$ ) of the powder. An example of the output of this program is shown in Figure 3.8.

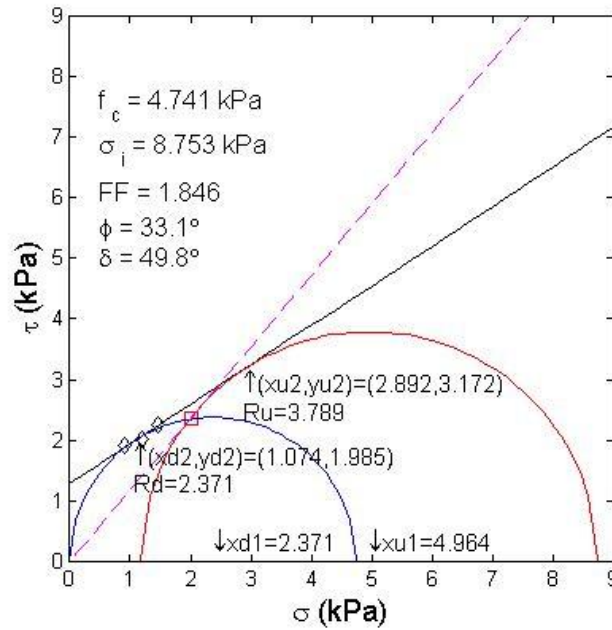


**Figure 3.8: Representative Graph of Shear Results**

The inverse slope of a plot of  $\sigma_i$  versus  $F_c$  is the Jenike flow index. The average Jenike flow index for the API was 2.18, which indicates a cohesive powder. Respirose® had an average Jenike flow index of 3.39, which also indicates a cohesive powder. However, the average Jenike flow index for the Respirose® powder had a standard deviation of 1.65, which indicates poor repeatability. This powder was very difficult to shear reliably, which supports claims by Bell [31] that shear tests can be difficult to perform.

The Jenike flow index of aspartame varied from 0.885 at 0.34% moisture content to a maximum of 4.39 at 4.98% moisture content, and then decreased back to 3.65 at 8.27% moisture content. Overall, the flowability improved from hardened to cohesive behaviour with an increase in moisture content. The aspartame powder was observed to form macroscopic round agglomerates. The increase in moisture content may increase the formation of these large spherical agglomerates, which improved the flowability of

the small, needle-shaped powder. The improvement in flowability declined as the moisture content reached 8%, probably due to the increased strength of liquid bridges between agglomerates.

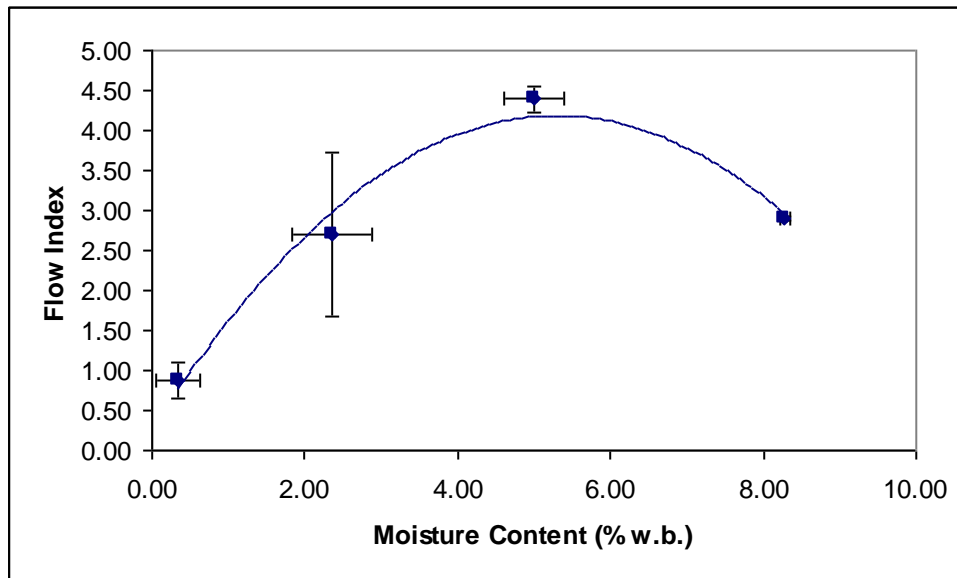


**Figure 3.9: Flow Index of Aspartame**

The Jenike flow index of HPMC varied with moisture content, though not in the predicted manner. The flow index decreased to a minimum of 1.63 at 5.01% moisture content, and then increased to 2.65 at 10.2% moisture content. According to these results, HPMC is cohesive at low and high moisture contents, but very cohesive at moderate moisture contents (i.e. 5%). The improvement in flowability beyond 5% moisture content may be caused by a lubricating effect of the surface moisture. This lubrication was also noted by Nokhodchi et al. [16] when performing compressibility tests on HPMC. Flowability first decreases as the moisture causes increased inter-particle forces, and then increases as surface asperities are covered by an increasingly thick layer of surface water.

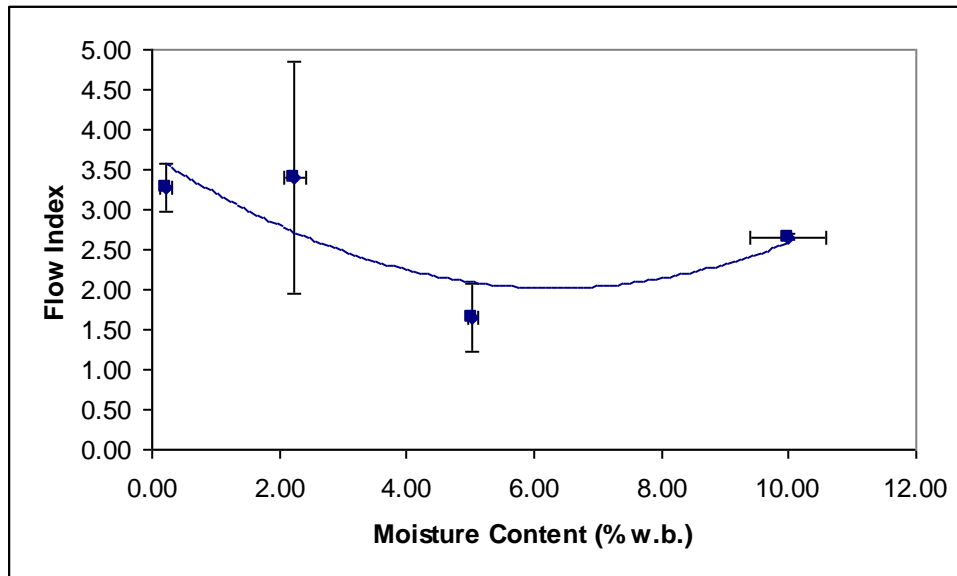


*Figure 3.10: Flow Index of HPMC*

### 3.4.5 Comparison of Flow Tests:

From previous research performed by Fitzpatrick et al. [5], it was expected that increasing moisture content would decrease the flowability of fine powders. Static angle of repose tests clearly showed a decrease in flowability as moisture content increased for aspartame, though not for HPMC. Dynamic angle of repose tests were inconclusive for both aspartame and HPMC. The Hausner Ratio and Carr Index showed a decrease in flowability with moisture content for aspartame, but no dependence on moisture content for HPMC. Meanwhile, shear tests showed an increase in flowability with increasing moisture content for aspartame and a decrease in flowability for HPMC.

Obviously, none of the other tests paralleled the results from the shear tests for aspartame. Neither was the decrease in flowability from cohesive to very cohesive and the return to cohesive behaviour of HPMC in the shear tests accurately reflected by the



Hausner Ratio, Carr Index or angle of repose tests. The effect of moisture on flowability is complex, and was not accurately captured by the “simple testers”.

### **3.5 Conclusions**

Increasing moisture content non-linearly decreased the flowability of HPMC, and non-linearly increased the flowability of aspartame. The so-called “simple testers” were not always an accurate predictor of the Jenike flow index for any of the pharmaceutical powders studied. For complex flow behaviour, like that of moist pharmaceutical powders, the Jenike shear test remains the only acceptable test of flowability.

### **3.6 Acknowledgement**

The author would like to thank Zhiguo Wang for the development of the Matlab® software used to interpret shear test results.

### **3.7 References**

- [1] R. Nelson, Why study particle science? 2006.
- [2] A. Bodhmag, Correlation between physical properties and flowability indicators for fine powders, (2006).
- [3] C. Dury, G. Ristow. Boundary effects on the angle of repose in rotating cylinders, The American Physical Society. 57 (1998) 4491-4497.
- [4] T.A. Bell. Industrial needs in solids flow for the 21<sup>st</sup> century, Powder Handling and Processing. 11 (1999) 9-12.

- [5] J. Fitzpatrick, S.A. Barringer, T. Iqbal. Flow property measurements of food powders and sensitivity of Jenike's hopper design methodology to the measured values, *Journal of Food Engineering*. 61 (2004) 399-405.
- [6] M.E. Plinke, D. Leitch, F. Loffler. Cohesion in granular materials, *Bulk Solids Handling*. 14 (1994) 101-106.
- [7] H. Abou-Chakra, U. Tüzün. Microstructural blending of coal to enhance flowability, *Powder Technology*. 111 (2000) 200-209.
- [8] G. Amidon. The effect of moisture on the mechanical and powder flow properties of microcrystalline cellulose, *Pharmaceutical Research*. 12 (1995) 923-929.
- [9] K. Chang, D. Kim, S. Kim, M. Jung. Bulk flow properties of model food powder at different water activity, *International Journal of Food Properties*. 1 (1998) 45-55.
- [10] M.C. Coelho, N. Harnby. The effect of humidity on the form of water retention in a powder, *Powder Technology*. 20 (1978) 197-200.
- [11] M.C. Coelho, N. Harnby. The effect of moisture on the equilibrium mixture quality of powders, *Powder Technology*. 23 (1979) 209-217.
- [12] T. Iqbal, J.J. Fitzpatrick. Effect of storage conditions on the wall friction characteristics of three food powders, *Journal of Food Engineering*. 72 (2006) 273-280.
- [13] E. Teunou, J.J. Fitzpatrick, E.C. Synnott. Characterization of food powder flowability, *Journal of Food Engineering*. 39 (1999) 31-37.
- [14] S. Kamath, V.M. Puri, H.B. Manbeck. Flow property measurement using the Jenike cell for wheat flour at various moisture contents and consolidation times, *Powder Technology*. 81 (1994) 293-297.
- [15] A. Nokhodchi, M.H. Rubinstein. The effect of moisture on the compaction properties of the binary mixture of hydroxypropyl methylcellulose K4M/ibuprofen, *S.T.P. Pharma Sci*. 8 (1998) 349-356.
- [16] A. Nokhodchi, M.H. Rubinstein. An overview of the effects of material and process variables on the compaction and compression properties of hydroxypropyl methylcellulose and ethylcellulose, *S.T.P. Pharma Sci*. 11 (2001) 195-202.

- [17] C. Dalton, B. Hancock. Processing and storage effect on water vapour sorption by some model pharmaceutical solid dosage formulations, *International Journal of Pharmaceuticals*. 156 (1997) 143-151.
- [18] G. Rowley, L.A. Mackin. The effect of moisture sorption on electrostatic charging of selected pharmaceutical excipient powders, *Powder Technology*. 135 (2003) 50-58. [15]
- [19] M. Stanford, C. DellaCorte. Effects of humidity on the flow characteristics of a composite plasma spray powder, *Journal of Thermal Spray Technology*. 15 (2006) 33-36.
- [20] J. Cain. An alternative technique for determining ANSI/CEMA Standard 550 flowability ratings for granular materials, *Powder Handling and Processing*. 14 (2002) 218-220.
- [21] R. Carr, Evaluating flow properties of solids, *Chemical Engineering*. 72 (1965) 163.
- [22] S. Marcus, G. Chaplin, T. Pugsley. The hydrodynamics of the high-density bottom zone in a CFB riser analyzed by means of electrical capacitance tomography (ECT), *Chemical Engineering Science*. 55 (2000) 4129-4138.
- [23] R. Hedge, J.L. Rheingold, S. Welch, C.T. Rhodes. Studies of powder flow using a recording powder flowmeter and measurement of the dynamic angle of repose, *Journal of Pharmaceutical Sciences*. 74 (1985) 11-15.
- [24] A. Drescher, A.J. Waters, C.A. Rhoades. Arching in hoppers: I. Arching theories and bulk material flow properties, *Powder Technology*. 84 (1995) 165-176.
- [25] J.L.P. Soh, C.V. Liew, P.W.S. Heng. New indices to characterize powder flow based on their avalanching behaviour, *Pharmaceutical development and technology*. 11 (2006) 93-102.
- [26] D.C. Abdullah, D. Geldart. The use of bulk density measurements as flowability indicators, *Powder Technology*. 102 (1999) 151-165.
- [27] K.M. Hill, J. Kakalios. Reversible axial segregation of binary mixtures of granular material, *Physical Review E*. 49 (1994) R3610-R3613.
- [28] A. Castellanos, J. Valverde, A. Perez, A. Ramos, P.K. Watson. Flow regimes in fine cohesive powders, *The America Physical Society*. 82 (1999) 1156-1159.

- [29] K. Yamane, T. Tanaka, Y. Tsuji, M. Nakagawa, S.A. Altobelli, DEM and MRI studies of particulate flows in a rotating cylinder; Flow visualization and image processing of multiphase systems, Flow Visualization and Image Processing of Multiphase Systems, FED (series) v.209 ed., ASME, 1995, pp. 225-228.
- [30] R.Y. Yang, R.P. Zou, A.B. Yu. Microdynamic analysis of particle flow in a horizontal rotating drum, Powder Technology. 130 (2003) 138-146.
- [31] T.A. Bell, Flowability measurement and interpretation in industry, Handbook of Conveying and Handling of Particulate Solids, 10th ed., 2001, pp. 3-13.

## **Chapter 4**

### **Introduction to the Effect of Size and Shape on Powder Flowability**

This chapter serves as a transition to the manuscript that describes research on the effect of shape and size on powder flowability. That manuscript, which constitutes Chapter 5 of this thesis, has been submitted for publication to Powder Technology and is currently undergoing peer review.

#### **Citation**

E. Emery, A. Bodhmag, J. Oliver, T. Pugsley, R. Tyler, J. Sharma, J. Zhou. Influence of shape and size on the flowability of pharmaceutical powders, Powder Technology. Submitted (2008). [1]

#### **4.1 Contribution of this Paper to the Overall Study**

This paper investigates the effect of particle shape and size on powder flowability. Five starch powders (barley, cow cockle, rice, rye and tapioca) were used. Additionally, previously unpublished data on the shape of selected pharmaceutical powders (aspartame, an active pharmaceutical ingredient (API), hydroxypropyl methylcellulose (HPMC) and Respitose® ML001) are combined with the starch results to give a more complete picture of the influence of particle shape and size on flowability. This research addresses objective #3 of the thesis.

#### **4.2 Contribution of the Master's Candidate**

Experiments were planned by Erica Emery and Todd Pugsley, and performed by Erica Emery and Jasmine Oliver. Additional experimental data from previous work by Abhaykumar Bodhmag was included. Bob Tyler and Jitendra Sharma were consulted

for advice on experimental procedures. All writing was done by Erica Emery, with editorial advice from Todd Pugsley, Jitendra Sharma, Bob Tyler and Joe Zhou (Eli Lilly).

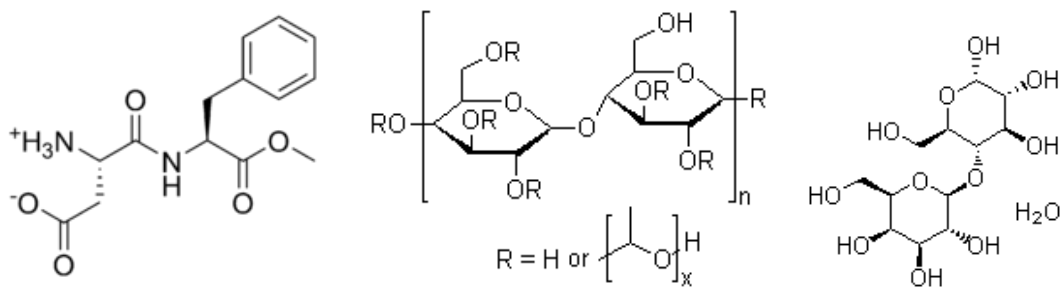
### **4.3 Background on Starches**

Starches are naturally occurring complex biopolymers, which occur in the form of granules. They come in a variety of shapes and sizes, depending on the plant of origin [2]. Rice starch granules are approximately 4  $\mu\text{m}$  in diameter [2-5] whereas rye starch granules are 22-36  $\mu\text{m}$ , and barley starch granules are 15-32  $\mu\text{m}$  [3]. Rice starch has irregular granules which allows them to agglomerate [6]. Rye and barley starch, on the other hand, are smooth and round and tend to exhibit bimodal size distributions [3]. Very little has been published on the surface morphologies of cow cockle and tapioca starch, but anecdotal evidence suggests both are small, smooth and round. There have been many studies on the rheology of starch solutions, but relatively little on the flowability of dry starch powders.

### **4.4 Background on Pharmaceutical Powders**

The same four pharmaceutical powders discussed in the previous paper (Chapter 3) were used here to investigate the effects of shape and size on flowability. Whereas the previous paper focused on moisture effects, results of this portion of the work may have been influenced by surface effects. While a complete study of surface effects is beyond the scope of the present study, structural formulas of the pharmaceutical powders tested are included for the sake of completeness in this transition Chapter 4.

Aspartame is a methyl ester of the dipeptide of the amino acids aspartic acid and phenylalanine. It has a molecular weight of 294.31 g/mole. Its chemical structure ( $C_{14}H_{18}N_2O_5$ ) is illustrated in Figure 4.1(a) [7]. Hydroxypropyl methylcellulose (HPMC) is used as a binder and as a retarding agent in many oral tablet and capsule formulations. For the specific powder used, DOW Methocel F, the degree of substitution of the hydroxypropyl group on the anhydroglucose units of cellulose was 1.9. Its chemical structure ( $C_6H_7O_2(OH)_x(OCH_3)_y(OC_3H_7)_z$   $x+y+z=3$ ) is illustrated in Figure 4.1(b) [8]. Respitose® ML001 is a trade name for  $\alpha$ -lactose monohydrate. It is a fine amorphous powder with a molecular weight of 360.31 g/mole. Its chemical structure ( $C_{12}H_{22}O_{11} \cdot H_2O$ ) is illustrated in Figure 4.1(c) [9]. The chemical formula for the active pharmaceutical ingredient (API) is proprietary information and will not be presented here.



a) *Aspartame*                      b) *HPMC*                      c) *Lactose Monohydrate*  
**Figure 4.1: Chemical formula of Pharmaceutical Powders (a) Aspartame, b) HPMC, c) Lactose Monohydrate)**

## 4.5 References

- [1] E. Emery, A. Bodhmag, J. Oliver, T. Pugsley, B. Tyler, J. Sharma, J.Zhou. Influence of shape and size on the flowability of pharmaceutical powders, Powder Technology. Submitted (2008).
- [2] E. Gregorova, W. Pabst, I. Bochavenko, Characterization of different starch types for their application in ceramic processing, Journal of the European Ceramic Society. 26 (2006) 1301.
- [3] J. Jane, T. Kasemsuwan, S. Leas, A. IA, H. Zobel, D. IL, J.F. Robyt, Anthology of starch granule morphology by scanning electron-microscopy, Die Stärke. 46 (1994) 121.
- [4] D. Cledat, S. Battu, R. Mokrini, P.J.P. Cardot, Rice starch granule characterization by flow cytometry scattering techniques hyphenated with sedimentation field-flow fractionation, Journal of chromatography. 1049 (2004) 131.
- [5] S. Srichuwong, T. Sunarti, T. Mishima, N. Isono, M. Hisamatsu, Starches from different botanical sources I: Contribution of amylopectin fine structure to thermal properties and enzyme digestibility, Carbohydrate Polymers. 60 (2005) 529.
- [6] J.L. Willett, Packing characteristics of starch granules, Cereal chemistry. 78 (2001) 64.
- [7] Aspartame, <http://en.wikipedia.org/wiki/Aspartame> (accessed June 2008).
- [8] Hydroxypropyl Methylcellulose, <http://www.chemblink.com/products/9004-65-3.htm> (accessed June 2008).
- [9] D-Lactose Monohydrate, <http://www.chemblink.com/products/9004-65-3.htm> (accessed June 2008).



## **Chapter 5**

### **Influence of Shape and Size on Flowability of Pharmaceutical Powders**

Erica Emery, Abhaykumar Bodhimage, Jasmine Oliver, Todd Pugsley, Robert Tyler,  
Jitendra Sharma  
University of Saskatchewan  
Joe Zhou,  
Eli Lilly

#### **5.1 Abstract**

Five starches (cow cockle, barley, rye, rice, and tapioca) as well as four pharmaceutical powders (aspartame, an active pharmaceutical ingredient, hydroxypropyl methylcellulose, and Respitose® ML001) were characterized with respect to particle shape and size, and then tested for their flowability. Powder flowability was measured using the Jenike shear test, the most widely accepted flowability standard in the pharmaceutical industry. It was found that the Jenike flow index decreased linearly with decreasing aspect ratio and decreasing roundness for the powders investigated. It was also determined that particle shape had a greater impact on flowability than did particle size for powders under 30  $\mu\text{m}$  in diameter.

#### **5.2 Introduction**

It has been reported that approximately 75% of chemical manufacturing processes involve particulate solids at some stage [1]. Transport, storage and handling of powders is especially important in the pharmaceutical industry, where nearly 80% of products are in solid dosage form [2] and the flow of fine powders of varying shapes and sizes from bins and hoppers into rapidly moving tablet presses is required. Process upsets,

inconsistent product quality and even complete process shutdowns are examples of major problems that can arise from erratic powder flow behaviour [2]. The flow properties of particulate solids and powders are known to depend on physical properties such as particle size and shape and particle size distribution [3, 4], as well as environmental properties such as moisture content and time-consolidation [2, 5-7]. According to Dury et al. [8], the behaviour of granular materials has been researched for over 200 years. Despite this, accurate prediction of powder flow behaviour based on physical properties is still not possible [9].

### **5.2.1 Size effects**

Finer powders tend to exhibit reduced flowability because of the greater surface area-to-mass ratio that allows cohesive surface forces to dominate over gravitational forces [10]. Both Teunou et al. [11] and Hedge et al. [4] reported an inverse relationship between angle of repose and powder size (the smaller the powder, the larger the angle of repose with a larger angle corresponding to more cohesive powder flow). Cain [12] found a strong relationship between mean powder diameter and Jenike flow factor, while Lahdenpaa et al. [13] stated that larger particles flowed more easily.

On the other hand, Fitzpatrick et al. [10] found no significant relationship between particle properties and powder flow index for food powders. Teunou et al. [11][14], when testing sugars and glass beads, found that the angle of internal friction increased with increasing particle size, even though the angle of repose decreased. In his experiments, Kaye [15] discovered that 15  $\mu\text{m}$  calcium carbonate powder exhibited

poorer flow than 1  $\mu\text{m}$  calcium carbonate powder, which was attributed to the smaller powder picking up moisture more easily and forming round agglomerates [15]. According to Freeman [16], “Flowability of a powder is not an inherent function of the physical powder but a consequence of the combined effects of many variables”.

### **5.2.2 Shape effects**

Powder shape also influences flowability. Shape and size are related, since shape is often described as a ratio of characteristic lengths [17]. Teunou et al. [11] found that the angle of repose was affected by the shape of sugar and glass particles. Powder shape determines the number of contact points between individual powder grains, which affects inter-particle forces [11, 18]. Iida [19] found that the flowability of cellulose increased with an increase in roundness. Many shape factors can be calculated in order to quantify powder shape, but according to Bodhmaghe [2], aspect ratio, roundness and irregularity are the most useful factors for describing pharmaceutical powders. Many of the other factors are simply variations of these three factors. In the current study, aspect ratio, roundness and irregularity were the factors used to describe particle shape. Their definitions are provided in Section 5.3.2.

### **5.2.3 Knowledge gap**

There is a need for better understanding of which physical properties affect powder flowability the most. Starch powders are ideal candidates for such a study because they occur naturally in a variety of shapes and sizes. This paper describes the results of a study of the effect of shape and size on powder flow using five starch powders (barley,

cow cockle, rice, rye and tapioca). Additionally, previously unpublished flowability data for selected pharmaceutical powders of varying shapes and sizes (aspartame, an active pharmaceutical ingredient (API), hydroxypropyl methylcellulose (HPMC), and Respitose® ML001) were combined with the starch results to develop a more complete picture of the relative importance of shape versus size on powder flowability.

## **5.3 Materials and Methods**

### **5.3.1 Powders Selected**

Starches are naturally occurring complex biopolymers which occur naturally in the shape of granules. Starch granules come in a variety of shapes and sizes, depending on the plant of origin [20]. Five starches were chosen for their range of granule shape and size, and for their availability. Rye starch was isolated from debranned rye using water and alcohol washes. First, the debranned rye was soaked in deionized water overnight. It was then ground with excess water in a kitchen blender. Following this the rye slurry was sieved through a 170-mesh (89µm opening) screen to remove coarse insolubles. The starch suspension which passed through the sieve was then centrifuged to remove excess water and the less dense protein top layer, which was scraped off. The starch was washed in deionized water and centrifuged several more times to ensure purity. Finally, the starch was washed in ethanol to remove the remaining water and then air dried. Barley starch was isolated from commercially available pearled barley in a similar manner.

Rice starch and tapioca starch were both purchased commercially from a local grocery store. Cow cockle (*Saponaria vaccaria*) starch was provided by Saponin Inc., Saskatoon, SK. The rice, tapioca and cow cockle starches were washed in ethanol to help remove impurities and to break up agglomerates.

The particular API used in the present study was provided by our industrial sponsor and had exhibited poor flowability in an industrial setting in the past. Aspartame is a commercially available sweetener that also tends to exhibit poor flow characteristics. Respitose® ML001 is a lactose monohydrate product commonly used as a pharmaceutical excipient. HPMC is a common pharmaceutical binding agent, as well as a retarding agent in solid dosage formulations. These four pharmaceutical powders were chosen because they are widely used in the industry and because they span a range of particle shapes and sizes.

### **5.3.2 Particle Characterization**

All powders investigated were characterized with respect to their size and shape. Some of the larger pharmaceutical powders, specifically HPMC and Respitose® ML001, were viewed using a stereomicroscope (Olympus SZ61, Center Valley, PA, USA) with an attached digital camera (Olympus DP12, Center Valley, PA, USA). The microscope was used to create 20 images, with approximately 500 particles detected in total, at a magnification of 90X. Approximately 15 scanning electron microscope (SEM) images were collected for each of the remaining powders, which were much finer and, therefore, could not be properly imaged using the stereomicroscope. The images were then

transferred to a personal computer for further image analysis. From the stereomicroscope and SEM images, approximately 500 particles were analysed using the Image-Pro Plus software (MediaCybernetics, Bethesda, MD, USA) to determine the particle descriptors of major and minor axis length, perimeter and projected area.

Aspect ratio, roundness, irregularity and equivalent circle diameter were calculated from these particle descriptors using equations 5.1-5.4 [2].

$$\text{Aspect Ratio} = \frac{b}{l} \quad (5.1)$$

$$\text{Roundness} = \frac{4 \times \pi \times A}{P^2} \quad (5.2)$$

$$\text{Irregularity} = \frac{P}{l} \quad (5.3)$$

$$\text{Equivalent Circle Diameter (ECD)} = 2 \times \sqrt{\frac{A}{\pi}} \quad (5.4)$$

In these equations  $b$  represents the length of the minor axis,  $l$  is the length of the major axis,  $A$  is the projected area, and  $P$  is the perimeter.

Aspect ratio varies between 0 and 1, with a low value indicative of an elongated particle; a perfect circle has an aspect ratio of 1. Roundness is a measure of how closely the projected area of the powder resembles a circle; a perfect circle has a roundness value of 1. Irregularity measures the surface area compared to the size of the particle; in this case, a perfect circle has an irregularity of  $\pi$ . Equivalent circle diameter (ECD) is a measure of size; it is the diameter of a sphere with the same cross-sectional area as the powder [2].

Powder flowability can be expressed in many different ways using one or more of the myriad of measurement techniques available [21, 22]. The Jenike flow index is generally accepted as the industry norm for determining the flowability of fine powders [9, 16, 22, 23]. From previous work done by our group, it was determined that only the Jenike flow index could accurately capture complex effects of the presence of moisture on powder flow behaviour [24]. Given our desire in the present work to isolate the effect of shape on powder flow, the Jenike index was employed. The flow index was determined from the results of several direct powder shear tests.

### **5.3.3 Shear tests:**

Direct shear tests involved two important steps: pre-shear and shear. The powder was loaded into the shear cell and consolidated at a relatively high load. Next, the powder was sheared at this same load, which is referred to as the pre-shear load. The load was then reduced to a fraction of the pre-shear load (20%, 50% or 80%) and shearing began. From a plot of shear stress at failure versus normal stress, it is possible to calculate the cohesion (y-intercept), the angle of internal friction (slope), and the yield locus [5, 25, 26].

From two Mohr's circles drawn tangent to the yield locus, the unconfined yield strength and major consolidating stress at each pre-shear load can be determined [10]. A plot of unconfined yield strength versus major consolidating stress is known as the Jenike flow function [10]. The flow index,  $ff_c$ , is the inverse of the slope of the flow function, and represents the strength of a consolidated powder that must be overcome before flow can

occur [5, 10]. A steep slope of the flow function corresponds to a cohesive powder with poor or difficult flow; a flat slope corresponds to smooth powder flow [5]. Flow becomes more difficult as one moves in an anti-clockwise direction on the flow function plot [10]. Table 5.1 presents rules-of-thumb that relate powder flowability to the flow index [10].

Table 5.1: Jenike classification of powder flowability by flow index ( $ff_c$ ) [10]

Flowability	Hardened	Very Cohesive	Cohesive	Easy Flow	Free Flow
Flow index	<1	<2	<4	<10	>10

The shear cell used in this study was a parallel plate direct shear cell, with a load cell calibrated for 0-100 N. It consisted of a 6 cm x 6 cm shear box connected to a motor, the load cell and a computer to record the output. The cross-sectional area of the shear cell before shear was  $3.546 \times 10^{-3} \text{ m}^2$ . It sheared at a fixed rate of 48 mm/hour. The cross-sectional area at any time is calculated by subtracting the distance travelled from the length of the side of the shear box. Three pre-shear loads were chosen based on ASTM Standard D 6128-00, which recommends pre-shear loads of 1.5 kPa, 3 kPa and 6 kPa for powders of low bulk density. Because of the range of weights available, the shear tests were actually performed with pre-shear normal loads of 1.60 kPa, 3.75 kPa and 5.60 kPa.

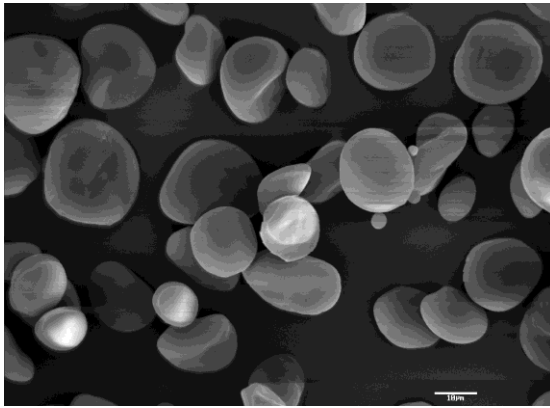
## 5.4 Results

### 5.4.1 Particle Characterization

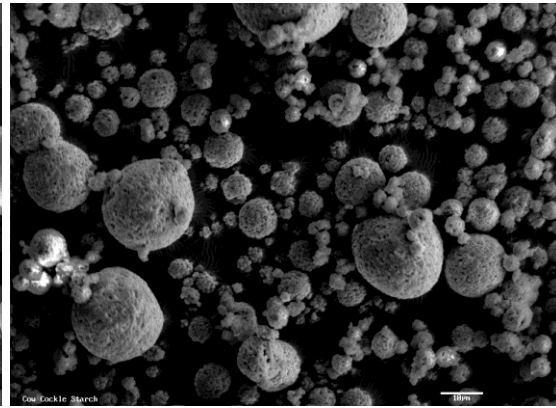
SEM images of the five starch powders are presented in Figure 5.1. Although the powders were very small, larger spherical agglomerates of cow cockle starch could be seen. Rice starch also had small particles that tended to agglomerate, although these were



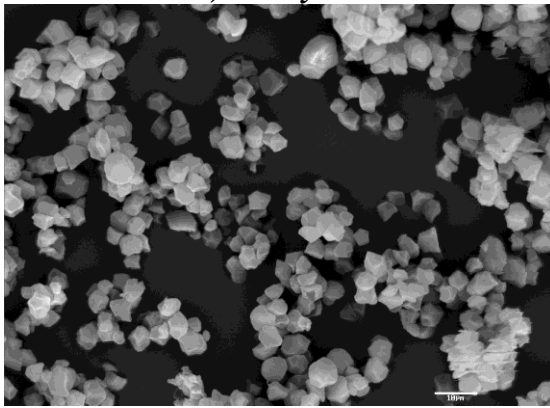
much more uneven. Some small particles remained in the rye and barley starch, but were outnumbered by the larger particles. The expected bi-modal distribution of barley and rye starches that has been reported in the literature [27] was almost non-existent. It was assumed that the smaller size cut had been lost during the washing, transferring and testing phases that the powders had undergone.



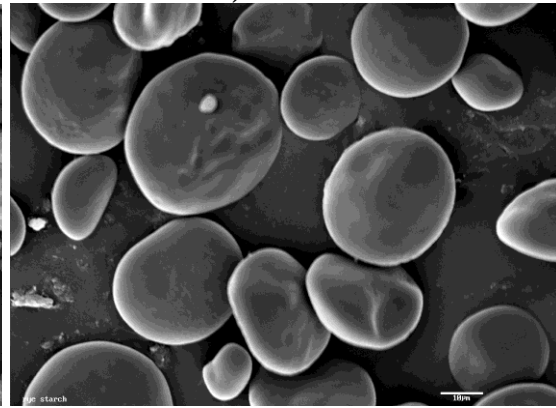
*a) Barley*



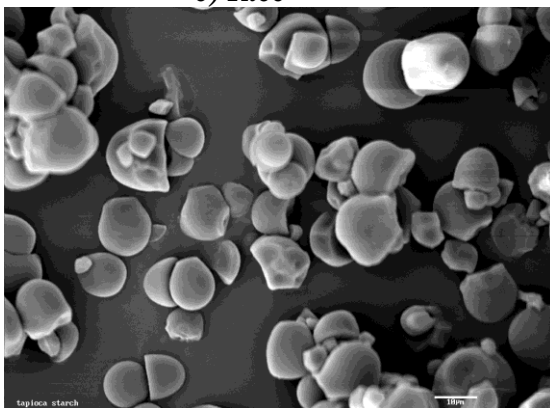
*b) Cow Cockle*



*c) Rice*



*d) Rye*



*d) Tapioca*

***Figure 5.1: Scanning Electron Microscope Images of Selected Starch Powders***

SEM also gives information about the shape and surface morphologies of the powders. Clearly, the rice starch was more irregular than the other starches. Although the individual grains of cow cockle starch were the smallest, the formation of large spherical agglomerates caused the average diameter to be slightly larger than that of rice. The resulting shape factors are listed in Table 5.2.

Table 5.2: Shape factors for selected starches

Powder	Aspect Ratio	Roundness	Irregularity	Equivalent Circle Diameter ( $\mu\text{m}$ )
Barley	0.720	0.910	2.767	14.4
Cow Cockle	0.859	0.868	3.121	5.2
Rice	0.785	0.871	2.955	4.4
Rye	0.762	0.906	2.851	22.5
Tapioca	0.837	0.926	2.969	10.0

SEM and stereomicroscopic images of the pharmaceutical powders are presented in Figure 5.2. The shape factors of the pharmaceutical powders were determined using the same technique as was used for the starch powders. Both the API and the aspartame were small needle-shaped powders and had the lowest aspect ratios of any of the powders investigated. HPMC and Respitose® both exhibited a high degree of irregularity; however, they were also much larger than the other powders. All of the pharmaceutical powders were less round than the starch powders. The shape factors of the pharmaceutical powders are summarized in Table 5.3.

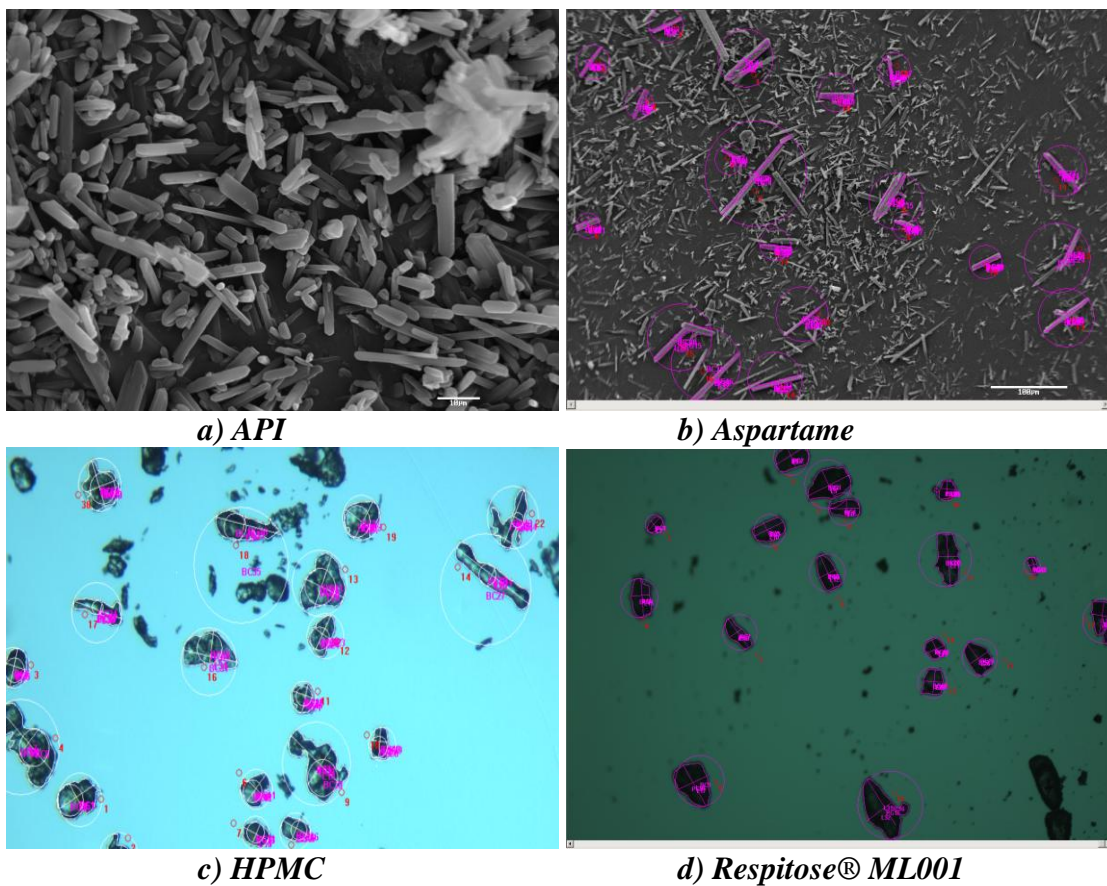


**Figure 5.2: Microscope and SEM images of Pharmaceutical Powders**

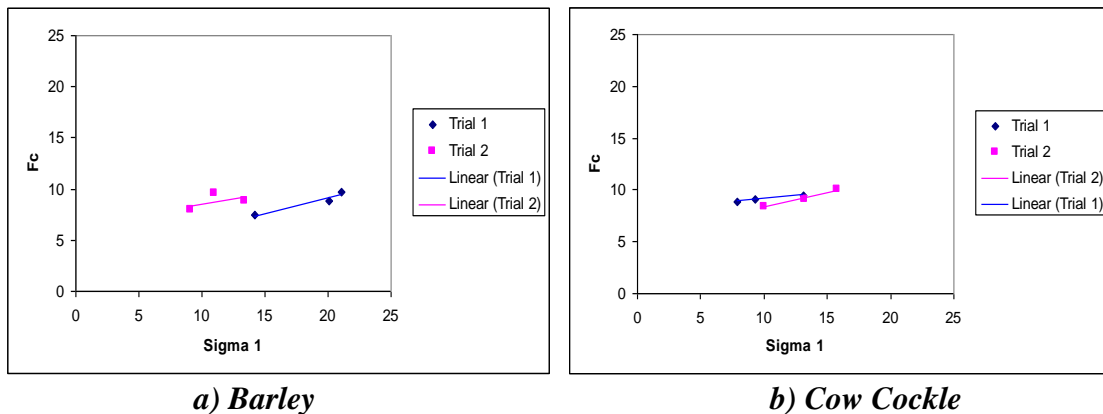
Table 5.3: Shape factors for selected pharmaceutical powders

Powder	Aspect Ratio	Roundness	Irregularity	Equivalent Circle Diameter ( $\mu\text{m}$ )
API	0.30	0.56	2.24	5.19
Aspartame	0.19	0.28	2.62	3.45
Respitose® ML001	0.63	0.70	3.96	56
HPMC	0.44	0.46	3.01	102

### 5.4.2 Shear Test Results

Analysis of direct shear test resulted in a flow function plot of unconfined yield strength ( $F_c$ ) versus major consolidating stress ( $\sigma_1$ ). The results for two trials of each starch powder are shown in Figure 5.3. The flow functions for all the starches were quite flat, corresponding to free flowing powders with large values of the Jenike flow index. As the slope of the flow function for tapioca starch was so close to zero, the flow index, which is the inverse of the flow function slope, exhibited high variability. Small changes in slope in this range caused large changes in the flow index.

Despite having the largest particle diameter and the lowest irregularity, barley and rye starches had the lowest Jenike flow indices of the starches, i.e. the worst flowability. Note, however, that these two starches also had the lowest aspect ratios, indicating elongated particles. From SEM images (Figure 5.1) we can see that these particles were plate-like, which corresponds to a more elongated particle and which may contribute to their poorer flowability.



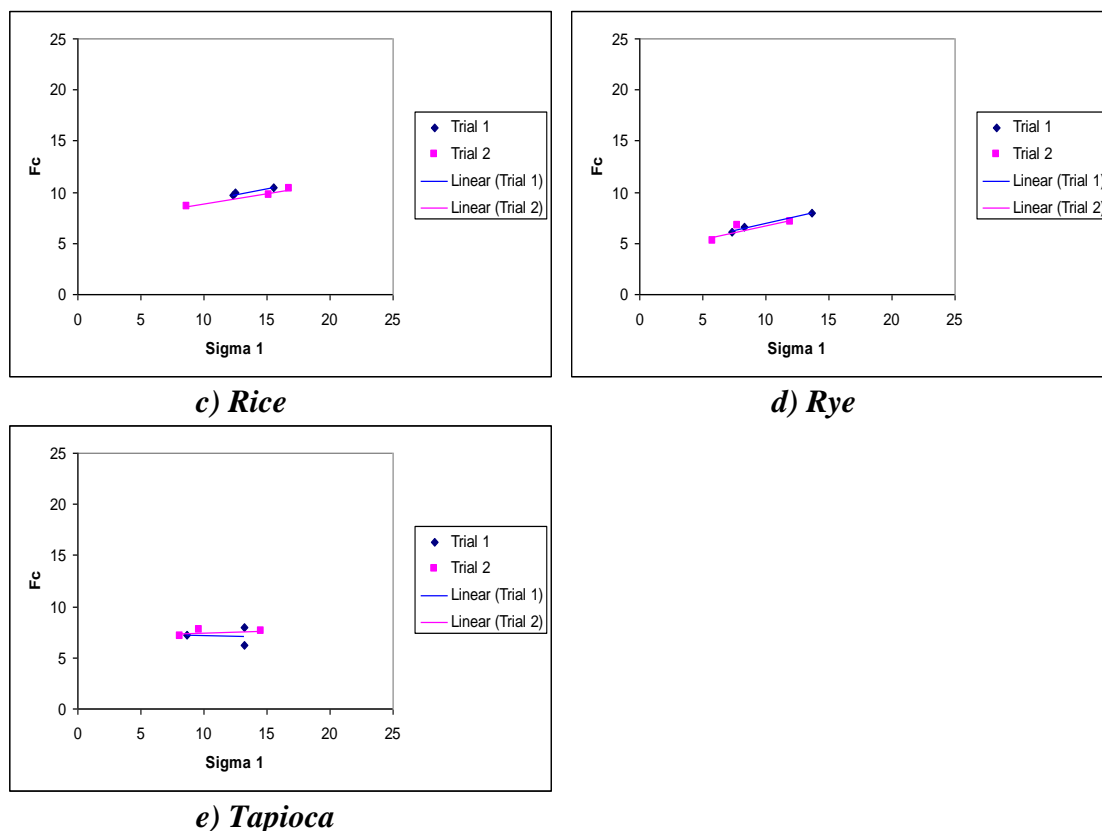


**Figure 5.3: Jenike Flow Function of Selected Starch Powders**

The results for two trials of each pharmaceutical powder are presented in Figure 5.4. Despite the similar sizes of the API, aspartame, cow cockle and rice powders, there was a large difference in their flowability. From the steep slope of the flow function (and corresponding low value of the flow index) for API and aspartame, it was concluded that these powders were cohesive. The flow functions of the starch powders more closely resembled the flow functions of the much larger Respitose® and HPMC powders. It is important to note that all powders were dried before testing to eliminate the effects of moisture content.

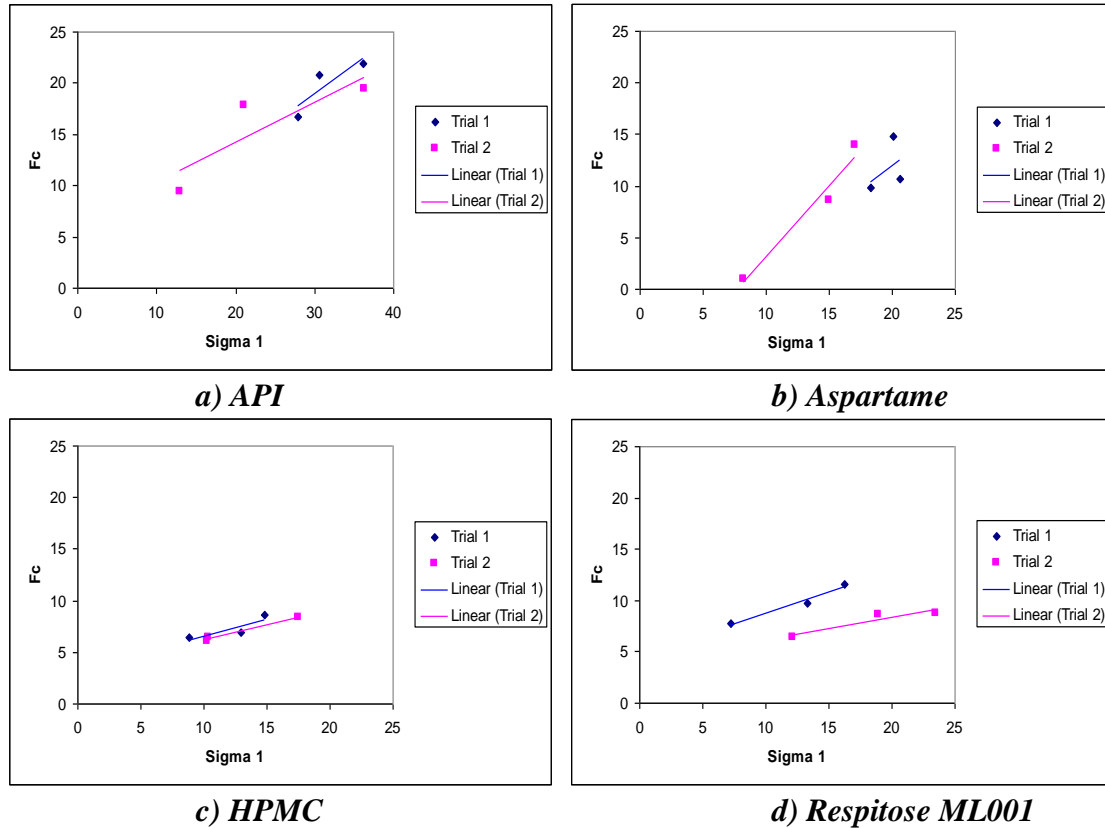


**Figure 5.4: Jenike Flow Function of Selected Pharmaceutical Powders (a) Aspartame, b) API, c) HPMC, d) Respitose ML001)**

The effects of particle shape and size on the Jenike flow index are shown in Figure 5.5. In these plots, the tapioca starch was excluded from the linear best-fit lines because of its high variability. From Figure 5.5(a), it can be seen that for the starch powders (represented by the solid black circles), there was a decreasing trend in the mean value of the Jenike flow index with increasing ECD. However, the high degree of variability in the shear tests noted above can be seen in the magnitude of the error bars. When this variability is taken into consideration, it would seem that there was little or no difference in the flowability of the four starch powders investigated. This is consistent with the summary presented in Table 5.3 for these starches, where it was seen that there was little

variation in the calculated shape factors. Visual observation of the starches also confirmed that they flowed quite easily their containers.

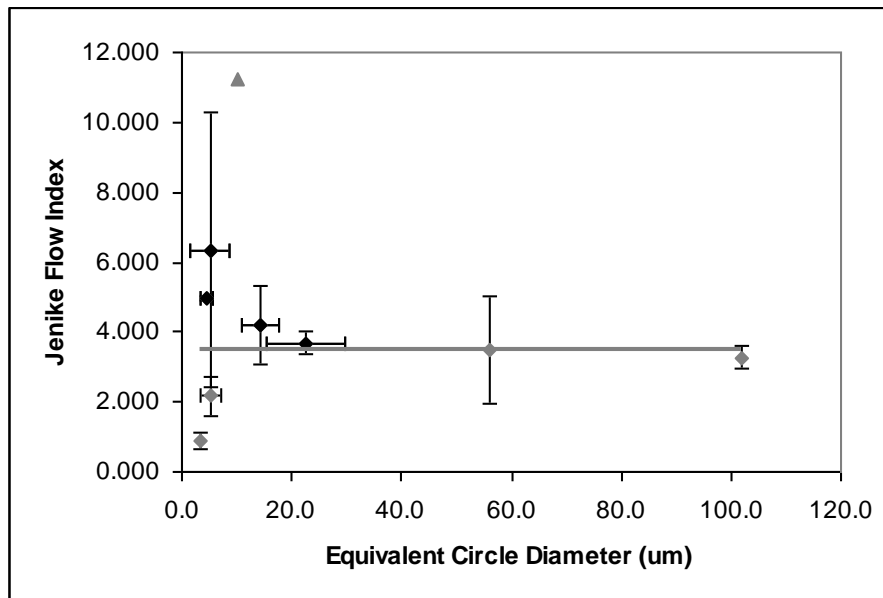
From further consideration of the pharmaceutical powders (represented by the grey diamonds in Figure 5.5a), it can be seen that the larger pharmaceutical powders (HPMC and Respitose® ML001) exhibited flow indices similar to those of the starches. The Jenike flow indices of the API and aspartame, on the other hand, were significantly less than those of the other powders, despite their similarity in size to the smallest starch powders which exhibited good flowability. The main difference between these powders is that aspartame and the API were needle-like in shape (low aspect ratio).

The influence of aspect ratio on powder flowability is illustrated in Figure 5.5(b) in the plot of Jenike flow index versus aspect ratio. The figure shows that powder flowability decreased as the aspect ratio decreased (i.e. as the powders become more elongated). A linear trend ( $R^2 = 0.85$ ) existed between aspect ratio and Jenike flow index. Unlike in Figure 5.5(a), the trend still held when the additional information from the pharmaceutical powders was added.

In considering Figure 5.5(c), which is a plot of Jenike flow index versus roundness, it is apparent that the starch results by themselves were inconclusive. This reflects the fact that the roundness values for the starches were all very similar. When the other pharmaceutical powder test results were added, a trend emerged. Jenike flow index improved linearly ( $R^2 = 0.66$ ) as the roundness approached one. The starch powders all

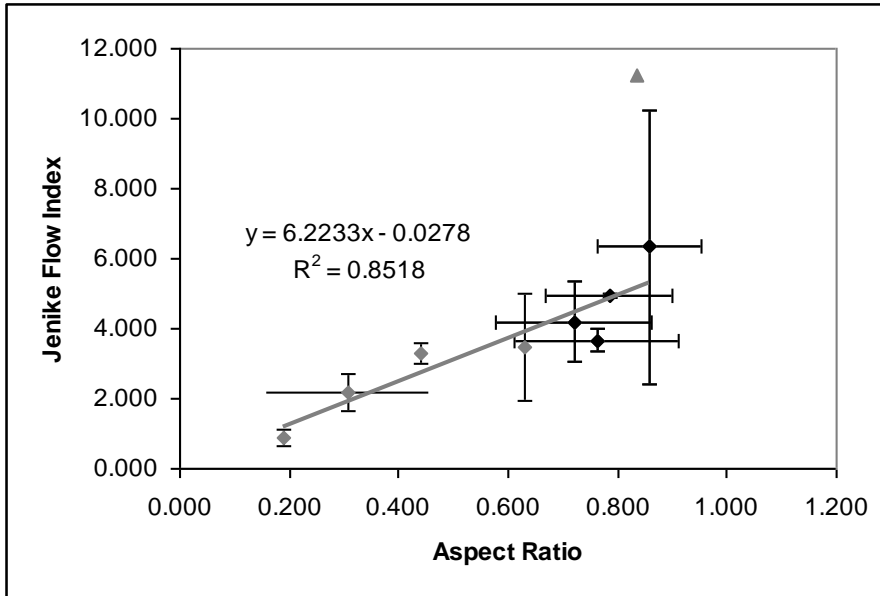
had higher roundness values than the pharmaceutical powders, providing another explanation for their superior flowability.

Figure 5.5(d) is a plot of Jenike flow index versus irregularity. Again, the high variability of the starch powders masked any indication of an overall trend. This time when the pharmaceutical powder results were added to the plot, no additional information was gained; there was no apparent relationship between irregularity and flowability.

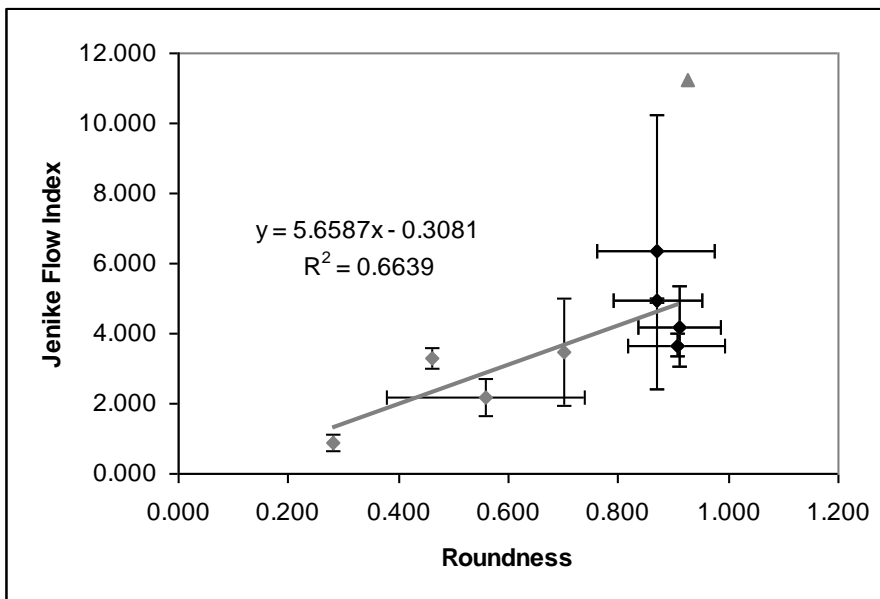


*a) Equivalent Circle Diameter*

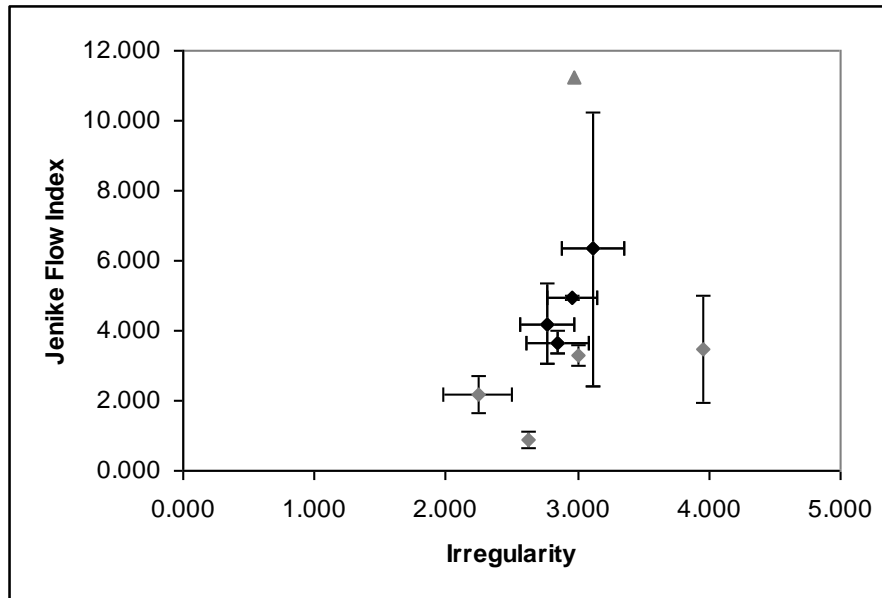




*b) Aspect Ratio*



*c) Roundness*



*d ) Irregularity*

**Figure 5.5: Effect of Size and Shape on Jenike Flow Index of Selected Powders (a) ECD, b) Aspect Ratio, c) Roundness, d) Irregularity)**

## 5.5 Conclusions

Although the starch powders were very small in size (under 30  $\mu\text{m}$  diameter), they flowed quite easily compared to the small pharmaceutical powders. Some property of the starch powders other than size affected their flowability. When the results from the pharmaceutical powders were considered, a more complete picture of the dependence of flowability on particle shape and size was gained. It appeared that aspect ratio was the property that affected the Jenike flow index the most. Roundness also had a linear relationship with the Jenike flow index, although with a slightly poorer fit. Aspect ratio describes the elongation of a particle and roundness represents the deviation from a perfect circle. Based on the powders investigated here, we concluded that powder shape, specifically the elongation of the powder, had the greatest effect on the flowability of fine pharmaceutical powders.

## 5.6 Nomenclature

$A$	area ( $\mu\text{m}^2$ )
$b$	minor axis ( $\mu\text{m}$ )
$ff_c$	Jenike flow index
$l$	major axis ( $\mu\text{m}$ )
$P$	perimeter ( $\mu\text{m}$ )
$F_C$	unconfined yield strength (kPa)
$\sigma_I$	major consolidating stress (kPa)

## 5.7 References

- [1] R. Nelson, Why study particle science? 2006.
- [2] A. Bodhmaghe, Correlation between physical properties and flowability Indicators for fine powders, (2006).
- [3] T.E. Durney, T.P. Meloy. Particle shape effects due to crushing method and size, International Journal of Mineral Processing. 16 (1986) 109-123.
- [4] R. Hedge, J.L. Rheingold, S. Welch, C.T. Rhodes. Studies of powder flow using a recording powder flowmeter and measurement of the dynamic angle of repose, Journal of Pharmaceutical Sciences. 74 (1985) 11-15.
- [5] H. Abou-Chakra, U. Tüzün. Microstructural blending of coal to enhance flowability, Powder Technology. 111 (2000) 200-209.
- [6] A. Castellanos, J. Valverde, A. Perez, A. Ramos, P.K. Watson. Flow regimes in fine cohesive powders, The American Physical Society. 82 (1999) 1156-1159.
- [7] M. Rhodes, Introduction to Particle Technology, John Wiley & Sons, Toronto, 1998.
- [8] C. Dury, G. Ristow. Boundary effects on the angle of repose in rotating cylinders, The American Physical Society. 57 (1998) 4491-4497.
- [9] T.A. Bell. Industrial needs in solids flow for the 21<sup>st</sup> century, Powder Handling and Processing. 11 (1999) 9-12.

- [10] J. Fitzpatrick, S.A. Barringer, T. Iqbal. Flow property measurements of food powders and sensitivity of Jenike's hopper design methodology to the measured values, *Journal of Food Engineering*. 61 (2004) 399-405.
- [11] E. Teunou, J. Vasseur, M. Krawczyk. Measurement and interpretation of bulk solids angle of repose for industrial process design, *Powder Handling and Processing*. 7 (1995) 219-227.
- [12] J. Cain. An alternative technique for determining ANSI/CEMA Standard 550 flowability ratings for granular materials, *Powder Handling and Processing*. 14 (2002) 218-220.
- [13] E. Lahdenpaa, M. Niskanen, J. Yliruusi. Study of some essential physical characteristics of three Avicel PH grades using a mixture design, *European Journal of Pharmaceutics and Biopharmaceutics*. 42 (1996) 177-182.
- [14] E. Teunou, J.J. Fitzpatrick, E.C. Synnott. Characterisation of food powder flowability, *Journal of Food Engineering*. 39 (1999) 31-37.
- [15] B.H. Kaye. Characterizing the flowability of a powder using the concepts of fractal geometry and chaos theory, *Particle & Particle System Characterisation*. 14 (1997) 53-66.
- [16] R. Freeman. The flowability of powders - an empirical approach, *International Conference on Powder & Bulk Solids Handling*. (2000).
- [17] M. Hentschel, N. Page. Selection of descriptors for particle shape characterization, *Particles and Particle Systems Characterization*. 20 (2003) 25-38.
- [18] M.E. Plinke, D. Leitch, F. Loffler. Cohesion in granular materials, *Bulk Solids Handling*. 14 (1994) 101-106.
- [19] K. Iida, K. Aoki, K. Danjo, A. Otsuka, C. Chen, E. Horisawa. A comparative evaluation of the mechanical properties of various celluloses, *Chemical Pharmaceutical Bulletin*. 45 (1997) 217-220.
- [20] E. Gregorova, W. Pabst, I. Bochavenko, Characterization of different starch types for their application in ceramic processing, *Journal of the European Ceramic Society*. 26 (2006) 1301.
- [21] T.A. Bell, Flowability measurement and interpretation in industry, *Handbook of Conveying and Handling of Particulate Solids*, 10th ed., 2001, pp. 3-13.

- [22] J. Fitzpatrick, L. Ahrné. Food powder handling and processing: Industry problems, knowledge barriers and research opportunities, *Chemical Engineering and Processing*. 44 (2005) 209-214.
- [23] A. Drescher, A.J. Waters, C.A. Rhoades. Arching in hoppers: I. Arching theories and bulk material flow properties, *Powder Technology*. 84 (1995) 165-176.
- [24] E. Emery, J. Oliver, T. Pugsley, J. Sharma, J. Zhou. The flowability of moist pharmaceutical powders, *Powder Technology*. submitted (2008).
- [25] S. Kamath, V.M. Puri, H.B. Manbeck. Flow property measurement using the Jenike cell for wheat flour at various moisture contents and consolidation times, *Powder Technology*. 81 (1994) 293-297.
- [26] K. Chang, D. Kim, S. Kim, M. Jung. Bulk flow properties of model food powder at different water activity, *International Journal of Food Properties*. 1 (1998) 45-55.
- [27] J. Jane, T. Kasemsuwan, S. Leas, A. IA, H. Zobel, D. IL, J.F. Robyt., Anthology of starch granule morphology by scanning electron-microscopy, *Die Stärke*. 46 (1994) 121.

## **Chapter 6**

### **Introduction to the Effect of Mixture Composition**

The following chapter (Chapter 7) is written in the form of a short publication. It has not been submitted for publication. The present transition chapter provides some additional information that was not included in the manuscript, as well as the contribution of this paper to the overall thesis topic.

#### **6.1 Contribution of this Paper to the Overall Study**

This paper addresses research objective #3; it investigates the effect of mixture composition on the flow of ordered mixtures of selected pharmaceutical powders.

#### **6.2 Contribution of the Master's Candidate**

Experiments were planned by Erica Emery and Todd Pugsley, and performed by Erica Emery and Jasmine Oliver (an undergraduate student who worked in the lab during the summer of 2007). Todd Pugsley and Jitendra Sharma were consulted for advice on experimental procedures. All writing was done by Erica Emery, with editorial advice from Todd Pugsley, Jitendra Sharma and Joe Zhou (Eli Lilly, the industrial partner in this work).

#### **6.3 Background on Ordered Mixtures**

Powder flowability is a complicated function of many factors, including particle properties and environmental properties. The behaviour of mixtures of powders is not

always a direct combination of the properties of the individual components [1]. Mixtures behave differently than single powders because the differently shaped and sized powders interact [2]. Small powders can coat the larger granules, decreasing inter-particle friction and increasing inter-particle distance, forming an ordered mixture [3]. Ordered mixtures of a small drug compound with a larger carrier powder are common to improve flowability [4].

#### 6.4 Additional Experimental Details

In order to effectively blend cohesive powders, which are known to have the potential to segregate during mixing, an Inversina mixer was purchased. The Inversina (Bioengineering, Wald, Switzerland) mixer subjects the powder to rotational, translational and inversion movements. This mimics manual shaking, thus providing highly effective blending without segregation. A mixing test was performed with Respitose® ML001 and a 1 cm placebo pharmaceutical granule. In the test, the two powders were mixed completely within 5 min at 50% power. Pictures of the powders before and after mixing are presented in Figure 6.1. This setting was used to create the ordered mixtures of pharmaceutical powders.

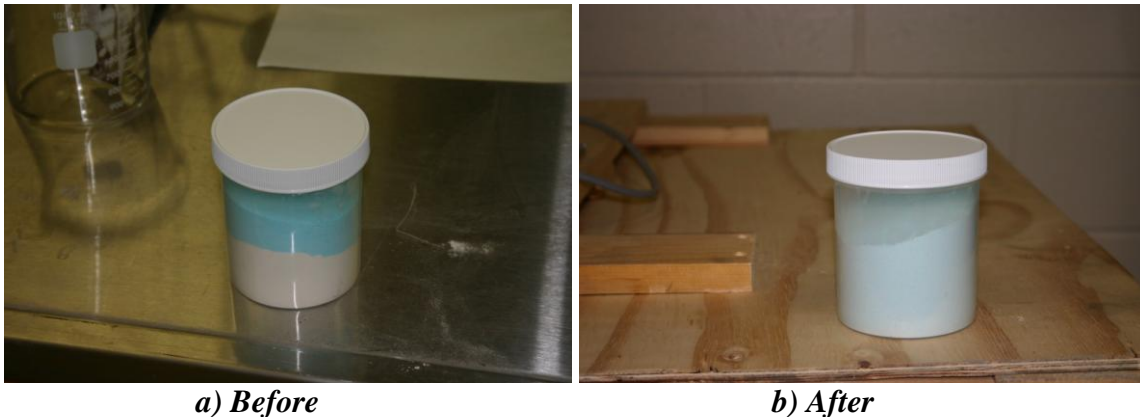


**Figure 6.1: Test of the Inversina Mixer (50% power for 5 minutes)**

## 6.5 References

- [1] U. Gohil, F. Podczek, N. Turnbull. Investigations into the use of pregelatinised starch to develop powder-filled hard capsules, *International Journal of Pharmaceutics*. 285 (2004) 51-63.
- [2] E. Lahdenpaa, M. Niskanen, J. Yliruusi. Study of some essential physical characteristics of three Avicel PH grades using a mixture design, *European Journal of Pharmaceutics and Biopharmaceutics*. 42 (1996) 177-182.
- [3] S. Jonat, S. Hasenzahl, M. Drechsler, P. Albers, K.G. Wagner, P.C. Schmidt, Investigation of compacted hydrophilic and hydrophobic colloidal silicon dioxides as glidants for pharmaceutical excipients, *Powder technology*. 141 (2004) 31.
- [4] K. Thalberg, D. Lindholm, A. Axelsson. Comparison of different flowability tests for powders for inhalation, *Powder Technology*. 146 (2006) 206-213.



## **Chapter 7**

### **Flowability of Ordered Mixtures**

Erica Emery, Jasmine Oliver, Todd Pugsley, Jitendra Sharma  
University of Saskatchewan  
Joe Zhou,  
Eli Lilly

#### **7.1 Abstract**

Ordered mixtures of pharmaceutical powders were examined to determine their flowability. Six combinations of Respitose® ML001, hydroxypropyl methylcellulose (HPMC), and an active pharmaceutical ingredient (API) in varying concentrations were investigated. Powder flowability was measured using the Jenike shear test, the most widely accepted flowability standard in the industry. The Jenike flow indices of the ordered mixtures were indistinguishable from the Jenike flow index of pure Respitose® at the  $\alpha = 0.1$  level.

#### **7.2 Introduction**

Transport, storage and handling of particulate solids are especially important in the pharmaceutical industry, where nearly 80% of products are in solid dosage form [1]. Uniform delivery of active drug ingredients is one of the most important considerations in the pharmaceutical industry [2, 3]. In order to ensure uniform delivery, the composition of the powdered mixtures that are compressed into tablets must be tightly controlled in order to maintain product quality. Failure of the tablets to meet product specifications can result in the rejection of batches worth millions of dollars. Maintaining smooth flow of powder mixtures out of storage hoppers and into tablet presses, therefore,

becomes very important. The flow properties of powders are known to depend on their particle shape, size and size distribution [2, 4], as well as environmental factors such as moisture content and time-consolidation [1, 5-7].

### **7.2.1 Glidants**

Despite research indicating that reduced powder size is associated with increased powder cohesion and, hence, poor flowability, adding controlled amounts of fine powders to a mixture doesn't necessarily reduce the flowability of the mixture. Glidants are fine powders (1-30  $\mu\text{m}$ ) added to many powder mixtures to improve flow properties [8-11]. There is some controversy over the exact mechanism, but two theories exist [9, 10]. The first is that small glidant powders coat the relatively larger host powders, increasing interparticle distance and decreasing interparticle forces [6, 9]. The second theory is that the glidant powders act in a manner analogous to ball-bearings, decreasing friction of rough surfaces [9]. Finely divided amorphous silica, silicon dioxide, and magnesium stearate are commonly used glidants [10, 12, 13].

### **7.2.2 Ordered Mixtures**

The term ordered mixture refers to a blend of pharmaceutical powders of specified composition with each powder having a well-defined role in the performance of the final blended product. For instance, the mixture will typically contain the active pharmaceutical ingredient (API) as well as a binder to give the tablet proper strength and excipients to assist with disintegration of the tablet and its uptake in the bloodstream after

it is ingested. The flowability of an active drug is often improved by adding larger particles to form an ordered mixture [14].

Prescott et al. [13] found that more effectively flowing blends could be achieved if one component of the mixture was cohesive or adhered to the surface of the other particles, forming an ordered mixture. Craik et al. [11] found the addition of 0.25%-0.5% magnesium oxide to an ordered mixture reduced the caking tendency of the mixture. Yuasa et al. [15] improved flowability of a mixture by adding starch, but decreased flowability when magnesium stearate was added. Abou-Chakra et al. [5] stated that flowability can be improved by optimising particle size distribution, but also stated that increased fines content leads to an increase in yield strength and a decrease in flowability. Ibqbal [16] also found that greater proportions of fines led to increased wall friction and decreased flowability.

Gold et al. [17] found flowability to pass through a maximum point when the fines content of a mixture increased. Yuasa et al. [15] stated that glidants were only effective when added in small quantities. In their study of ordered mixtures, Thalberg et al. [14], using micronized lactose as a stand-in for an actual API, found a decrease in flowability with an increase in micronized lactose, but not to the extent predicted by combining the flow properties of the individual components. However, the round micronized lactose particles did not completely reflect the behaviour of a true API, which tends to be more needle-shaped [14].

### 7.2.3 Knowledge gap

To date there have been several papers published on the flowability of ordered mixtures and on the effect of glidants. However none have studied ordered mixtures where the finest powder was a needle-shaped API. The objective of the present study was to determine the effect of composition on the flow of ordered mixtures of pharmaceutical powders containing an actual API.

## 7.3 Materials and Methods

### 7.3.1 Mixtures Selected

The particular API that was used was approximately 5.2  $\mu\text{m}$  in diameter and needle-shaped. It has exhibited poor flowability in an industrial setting in the past. Respitose® ML001 ( $\text{C}_{12}\text{H}_{22}\text{O}_{11} \cdot \text{H}_2\text{O}$ ) is a lactose monohydrate product, which is the most widely used excipient for inhalation [14]. It is approximately 56  $\mu\text{m}$  in diameter and round in shape. HPMC ( $\text{C}_6\text{H}_7\text{O}_2(\text{OH})_x(\text{OCH}_3)_y(\text{OC}_3\text{H}_7)_z$   $x+y+z=3$ ) is a common pharmaceutical binding agent, as well as a retarding agent in solid dosage formulations [18]. It is much larger with a diameter of 102  $\mu\text{m}$  and is slightly less round than Respitose®. These powders were chosen because they are widely used in formulation and they span a range of particle shapes and sizes.

According to Kono et al. [12] glidants are most effective in improving flowability when added in very small amounts. They experimented with flow conditioners in the range 0.1-5 wt% [12]. Thalberg et al. [14] varied the concentration of micronized lactose in the

range of 2.5-10% w/w. The compositions tested in this study are described in Table 7.1. In actual pharmaceutical formulations, the API is typically present in small concentrations in the overall mixture. Binders and excipients, such as HPMC and Respitose®, make up the balance of the mixture. The compositions below were chosen because they represent industrially relevant concentrations of pharmaceutical powders in ordered mixtures.

Table 7.1: Dry powder composition of ordered mixtures

Mixture No.	1	2	3	4	5	6
Respitose®	100	95	95	95	90	85
HPMC wt%	0	5	2.5	0	5	5
API wt%	0	0	2.5	5	5	10

### 7.3.2 Powder Flow Tests

Powder flowability can be expressed in many different ways using one or more of the myriad of measurement techniques available [19-21]. Jenike flow index is the most widely accepted method for describing flowability of fine powders [20, 22-25]. The Jenike flow index is determined from the results of several direct shear tests. The technique used to measure and interpret the Jenike flow index has been described previously in Emery et al. [23] and is also widely reported in the open literature and ASTM standards. For the sake of brevity, its description will not be included in the present paper.

### 7.3.3 Inversina Mixer

In order to effectively blend powders of widely varying shapes and size, which are known to have the potential to segregate during mixing, an Inversina (Bioengineering, Wald, Switzerland) mixer was utilized. The Inversina mixer is different from more standard pharmaceutical mixers, such as the V-blender or ribbon blender, because it subjects the powder to rotational, translational and inversion motion. This mimics manual shaking, thus providing highly effective blending without segregation. The Inversina mixer was used to create the ordered mixtures of pharmaceutical powders shown in Table 7.1.

## 7.4 Results

Shear tests were performed for each of the six ordered mixtures, the results of which are summarized in Figure 7.1. The plotted results are averages of two tests, with the error bars representing one standard deviation. Based on the average value of the flow index, the pure Respitose® and Ordered Mixture #6 (85/5/10::Respitose®/HPMC/API) exhibited the best flowability, although based on well-established rules-of-thumb for interpreting shear test results, both would be classified as cohesive since their flow indices were less than 4. Ordered Mixture #3 (95/2.5/2.5) had the poorest flowability and was classified as very cohesive. However, when the standard deviation of the results is taken into account using Student's t-test, none of the Jenike flow indices of the ordered mixtures was found to exhibit a statistically significant difference from the Jenike flow index of pure Respitose® at an  $\alpha = 0.1$  level of significance.

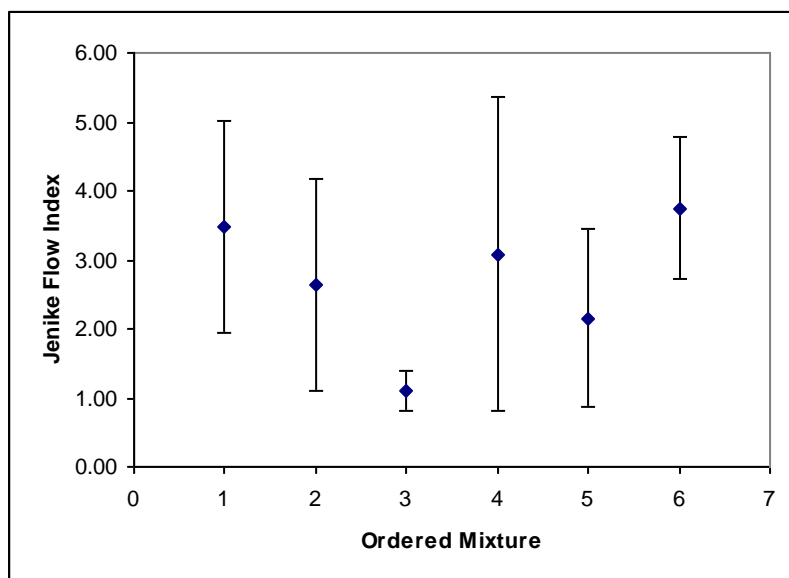


**Figure 7.1: Jenike Flow Index of Ordered Mixtures**

If the significance level is relaxed to  $\alpha = 0.5$  (0.25 in each tail of the two-tailed t test) some general trends emerge. The flowability of the ordered mixtures initially decreased then increased as the percentage of API in the mixture increased, as seen in Figure 7.2(a). Mixtures with less than 5% API exhibited poorer flow characteristics than mixtures with no API at all, but at 10% API, the mixture flowability was indistinguishable from the flowability of the 0% API cases.

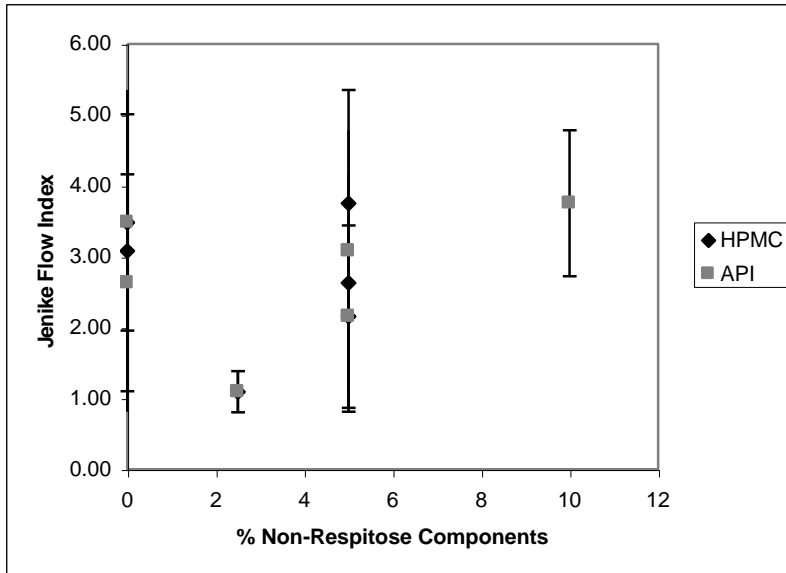
The flowability of Ordered Mixture #3, which contains Respitose®, API and HPMC, was significantly lower than that of mixtures containing only Respitose® and HPMC (OM #2) or Respitose® and the API (OM #4). Interestingly, the Jenike flow index of Ordered Mixture #3 was also significantly lower than the flow index of pure API as reported in Emery et al. [23] at the  $\alpha = 0.5$  level (but not at the  $\alpha = 0.1$  level). This may indicate that the interaction of the components is important, as well as their proportions. Even though

the larger and relatively easy-flowing HPMC was present in the same concentrations as the API, the flowability of the mixture was controlled by the smaller, more cohesive powder.

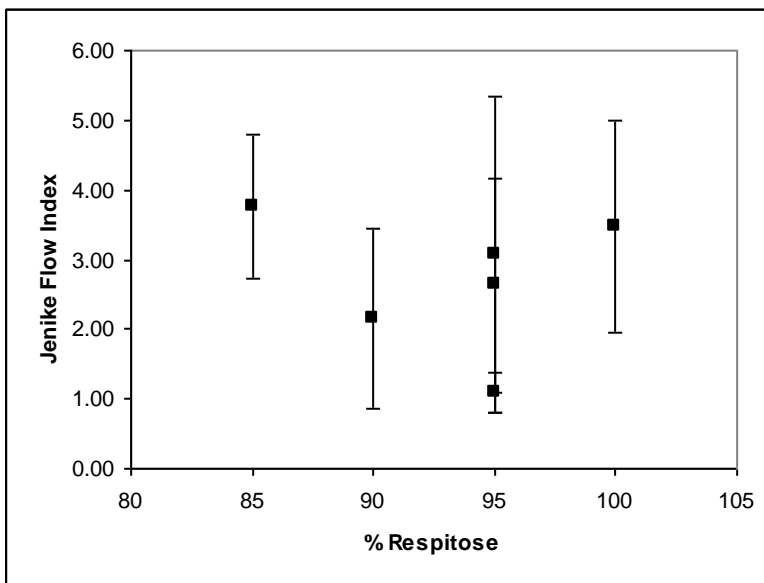
The observed improvements in flowability with changes in concentration may be caused by an optimization of the particle size distribution, as suggested by Abou-Chakra et al. [5]. API particles were an order of magnitude smaller than the Respitose® particles, whereas HPMC particles were twice as large. The flowability may also be improved by an agglomeration effect. In a previous paper [26], the authors found that this particular API had very poor flowability due to its elongated shape. If spherical agglomerates of API and another component (either Respitose® or HPMC) were to form, the flowability would improve.

No trend is discernable in Figure 7.2(b), which illustrates the effect of Respitose® content on Jenike flow index. In another previous paper [23], the authors found Respitose® to be difficult to shear reliably, with large variations in the Jenike flow index. This continues to be the case with ordered mixtures of Respitose®.





*a) Fines*



*b) Respitose®*

**Figure 7.2: Effect of Fines Content on Jenike Flow Index of Ordered Mixtures**

## 7.5 Conclusions

The Jenike flow index was used to define flowability for the ordered mixtures of pharmaceutical powders. Initially, adding small concentrations of API severely restricted flow, despite the presence of larger, easier flowing powders. At larger proportions of the

API (i.e. >5%), the flowability of the mixtures was improved. This may be due to the increased size distribution of the mixture or due to the formation of spherical agglomerates. The needle-shaped API did not behave as a typical glidant at low concentrations, reinforcing that actual pharmaceutical ingredients behave differently than round, easy-flowing flow additives. However, at the  $\alpha = 0.1$  level of significance, there was no difference in the Jenike flow indices of the ordered mixtures, so no conclusions could be drawn.

## 7.6 References

- [1] A. Bodhimage, Correlation between physical properties and flowability indicators for fine powders, (2006).
- [2] R. Hedge, J.L. Rheingold, S. Welch, C.T. Rhodes. Studies of powder flow using a recording powder flowmeter and measurement of the dynamic angle of repose, *Journal of Pharmaceutical Sciences*. 74 (1985) 11-15.
- [3] M. Mullarney, B. Hancock, G. Carlson, D. Ladipo, B. Langdon. The powder flow and compact mechanical properties of sucrose and three high-intensity sweeteners used in chewable tablets, *International Journal of Pharmaceutics*. 257 (2003) 227-236.
- [4] T.E. Durney, T.P. Meloy. Particle shape effects due to crushing method and size, *International Journal of Mineral Processing*. 16 (1986) 109-123.
- [5] H. Abou-Chakra, U. Tüzün. Microstructural blending of coal to enhance flowability, *Powder Technology*. 111 (2000) 200-209.
- [6] A. Castellanos, J. Valverde, A. Perez, A. Ramos, P.K. Watson. Flow regimes in fine cohesive powders, *The American Physical Society*. 82 (1999) 1156-1159.
- [7] M. Rhodes, *Introduction to Particle Technology*, John Wiley & Sons, Toronto, 1998.

- [8] E. Lahdenpaa, M. Niskanen, J. Yliruusi. Study of some essential physical characteristics of three Avicel PH grades using a mixture design, *European Journal of Pharmaceutics and Biopharmaceutics*. 42 (1996) 177-182.
- [9] S. Jonat, S. Hasenzahl, M. Drechsler, P. Albers, K.G. Wagner, P.C. Schmidt, Investigation of compacted hydrophilic and hydrophobic colloidal silicon dioxides as glidants for pharmaceutical excipients, *Powder technology*. 141 (2004) 31.
- [10] B.H. Kaye. Characterizing the flowability of a powder using the concepts of fractal geometry and chaos theory, *Particle & Particle System Characterisation*. 14 (1997) 53-66.
- [11] D.J. Craik, B.F. Miller, The flow properties of powders under humid conditions, *From the Plant Laboratory, Boots Pure Drug Co., Ltd.* (1958) 136T-144T.
- [12] H.O. Kono, C.C. Huang, M. Xi. Function and mechanism of flow conditioners under various loading pressure conditions in bulk powders, *Powder Technology*. 63 (1990) 81-86.
- [13] J. Prescott, R. Barnum. On powder flowability, *Pharmaceutical Technology*. 24 (2000) 60-84.
- [14] K. Thalberg, D. Lindholm, A. Axelsson. Comparison of different flowability tests for powders for inhalation, *Powder Technology*. 146 (2006) 206-213.
- [15] Y. Yuasa, M. Yamashiro. Experiments relating to fluidity and bulk density of powder solids with glidants addition, *Journal of Powder & Bulk Solids Technology*. 8 (1984) 19-22.
- [16] T. Iqbal, J.J. Fitzpatrick. Effect of storage conditions on the wall friction characteristics of three food powders, *Journal of Food Engineering*. 72 (2006) 273-280.
- [17] G. Gold, R.N. Duvall, B.T. Palermo, J.G. Slater. Powder flow studies III: Factors affecting the flow of lactose granules, *Journal of Pharmaceutical Sciences*. 57 (1968) 667-671.
- [18] A. Nokhodchi, M.H. Rubinstein. An overview of the effects of material and process variables on the compaction and compression properties of hydroxypropyl methylcellulose and ethylcellulose, *S.T.P. Pharma Sci*. 11 (2001) 195-202.
- [19] T.A. Bell, Flowability measurement and interpretation in industry, *Handbook of Conveying and Handling of Particulate Solids*, 10th ed., 2001, pp. 3-13.

- [20] J. Fitzpatrick, S.A. Barringer, T. Iqbal. Flow property measurements of food powders and sensitivity of Jenike's hopper design methodology to the measured values, *Journal of Food Engineering*. 61 (2004) 399-405.
- [21] J. Fitzpatrick, L. Ahrné. Food powder handling and processing: Industry problems, knowledge barriers and research opportunities, *Chemical Engineering and Processing*. 44 (2005) 209-214.
- [22] R. Freeman. The flowability of powders - an empirical approach, *International Conference on Powder & Bulk Solids Handling*. (2000).
- [23] E. Emery, J. Oliver, T. Pugsley, J. Sharma, J. Zhou. The flowability of moist pharmaceutical powders, *Powder Technology*. submitted (2008).
- [24] T.A. Bell. Industrial needs in solids flow for the 21<sup>st</sup> century, *Powder Handling and Processing*. 11 (1999) 9-12.
- [25] A. Drescher, A.J. Waters, C.A. Rhoades. Arching in hoppers: I. Arching theories and bulk material flow properties, *Powder Technology*. 84 (1995) 165-176.
- [26] E. Emery, A. Bodhmagé, J. Oliver, T. Pugsley, R. Tyler, J. Sharma, J. Zhou. Influence of shape and size on the flowability of pharmaceutical powders, *Powder Technology*. Submitted (2008).

## **Chapter 8**

### **Conclusions**

This research had four objectives: 1. To determine the effect of moisture content on the flow of selected pharmaceutical powders. 2. To study the effect of particle shape and size on powder flow using starch powders. 3. To determine the effect of composition on the flow of ordered mixtures of selected pharmaceutical powders. 4. To develop a novel flowability tester based on electrical capacitance tomography (ECT) that measures the dynamic angle of repose of powders. The conclusions drawn about each of these topics are presented in the following sections.

#### **8.1 Effect of Moisture Content**

The Jenike flow index of aspartame increased with an increase in moisture content. The aspartame powder had a tendency to form agglomerates that were round in shape. The increase in moisture content may have increased the formation of large spherical agglomerates, which improved the flowability of this small, needle-shaped powder. The increase in flowability was reduced as the moisture content reached 8%, probably due to the increased strength of liquid bridges between agglomerates.

The Jenike flow index of HPMC first decreased as increasing moisture content caused increased inter-particle forces, and then improved as an increasingly thick layer of surface water covered surface asperities. The increase in flowability of HPMC above 5% moisture content may have been caused by a lubricating effect of the surface moisture.

The flowability of the API was characterized as cohesive by the static angle of repose, Hausner Ratio and Carr Index tests, and as very cohesive by the shear tests. The flowability of Respitose® was characterised as cohesive by the dynamic angle of repose, Hausner Ratio and Carr Index tests, and as very cohesive by the static angle of repose and shear tests. The effect of moisture content on flowability is complex, and was only accurately captured by the Jenike flow index.

## **8.2 Effect of Particle Shape and Size**

Although the starch powders were very small in size (under 30 µm diameter), they flowed quite easily compared to the other small pharmaceutical powders. This phenomenon was confirmed visually while transferring the powder to the shear cell. The size of the powders did not dictate their flowability.

It appeared that aspect ratio was the property that affected the Jenike flow index the most ( $R^2 = 0.85$ ). Roundness also exhibited a linear relationship with the Jenike flow index, though with a slightly worse fit ( $R^2 = 0.66$ ). Aspect ratio describes the elongation of a particle and roundness represents the deviation from a perfect circle. It is concluded from the data that powder shape, specifically the elongation of the powder, had the greatest effect on the flowability of fine pharmaceutical powders.

## **8.3 Effect of Fines Content (Ordered Mixtures)**

The Jenike flow index was used to define the flowability for six ordered mixtures of pharmaceutical powders. There was no significant difference between the flow indices of

any of the ordered mixtures at the  $\alpha = 0.1$  level. The flowability of Ordered Mixture #3, which contained Respitose®, API and HPMC, was significantly lower than that of mixtures containing only Respitose® and HPMC (OM #2) or Respitose® and the API (OM #4) at the  $\alpha = 0.5$  level. Initially, adding small concentrations of API severely restricted flow, despite the presence of larger, easier flowing powders. Even though the larger and relatively easy-flowing HPMC was present in the same concentrations as the API, the flowability of the mixture is controlled by the smaller, more cohesive powder.

At larger proportions of the API (i.e. >5%), the flowability of the mixtures was improved. There are two theories to explain this startling result: 1) adding more of the small API optimized the size distribution, increasing flowability, and 2) the pharmaceutical powders interacted to form spherical agglomerates. Neither theory has been confirmed. The needle-shaped API did not behave as a typical glidant at low concentrations, reinforcing the belief that actual pharmaceutical ingredients behave differently than round, easy-flowing flow additives.

#### **8.4 Comparison of Flow Tests (Novel Dynamic Angle of Repose Tester)**

In the effect of moisture content experiments, the dynamic angle of repose tests were inconclusive for both aspartame and HPMC. Meanwhile, shear tests showed an increase in flowability with increasing moisture content for aspartame and a decrease in flowability for HPMC.

The novel dynamic angle of repose tester, which uses electrical capacitance tomography to view the center of a rotating cylinder, did not correlate well with the Jenike flow index. The novel dynamic angle of repose tester needs to be made more reproducible before it can be compared to the Jenike shear test. For complex flow behaviour, the Jenike shear test remains the only acceptable test of flowability.

## **8.5 Recommendations**

There are several practical recommendations resulting from this research. Since it was determined that increasing moisture content has different effects on different powders, it is recommended to investigate the behaviour of moist powders of interest individually, using the Jenike flow index. Other “simple” flowability testers are not recommended, since they did not adequately describe the complex flow behaviour of moist powders. Increasing the roundness and decreasing elongation of small powders is recommended to improve their flow properties.

The ECT dynamic angle of repose machine is not yet ready for industrial use. Further studies on the effect of wall surface, rotation speed and fill percentage are recommended. It is also recommended to create a user-independent method of calculating the dynamic angle of repose from the output images. Once these studies are complete the ECT dynamic angle of repose tester will be a reproducible and accurate device for the measurement of dynamic flow properties.



## Appendix A: Compressibility Test Results

The figures below show typical results from the tapped density tests performed on the pharmaceutical powders. Only one test is shown for each powder moisture content. A total of three tests were averaged to obtain the values reported in Chapter 3.

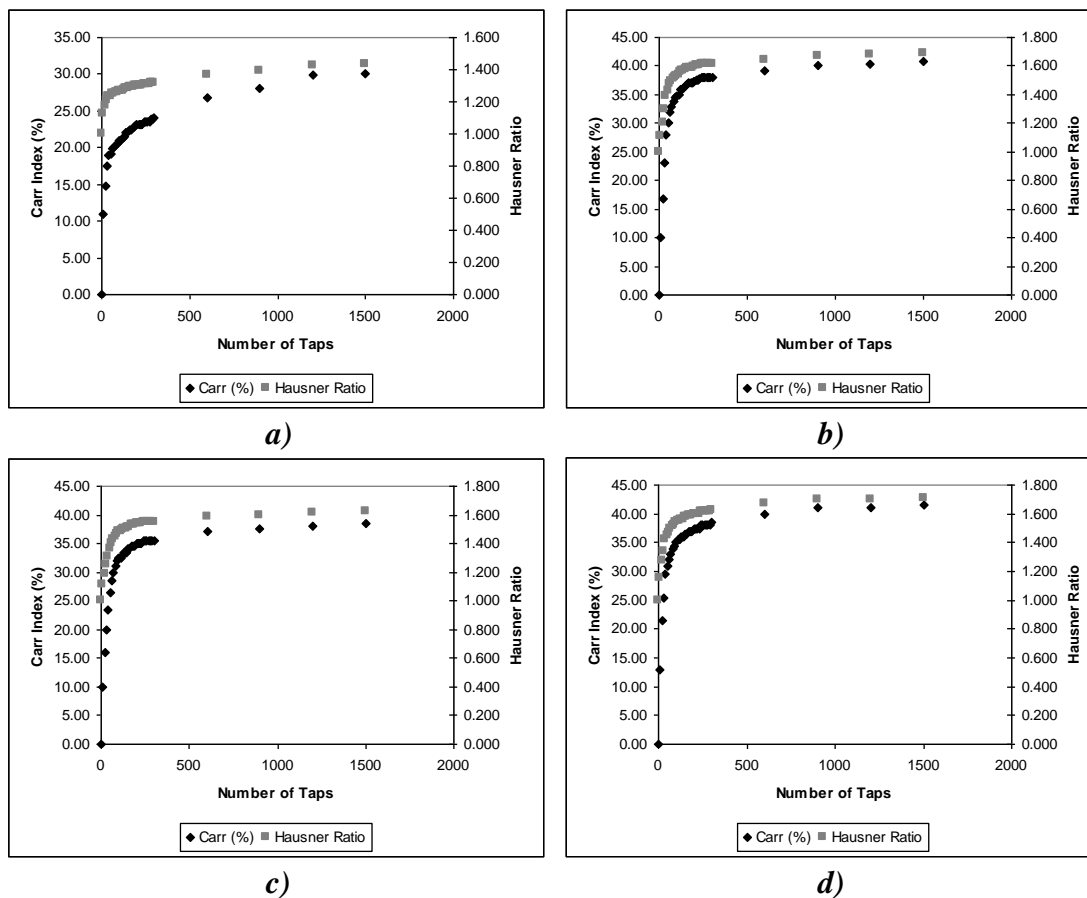


**Figure A.1: Compressibility of Aspartame at (a) 0%, (b) 2%, (c) 5%, (d) 8% Moisture Content**

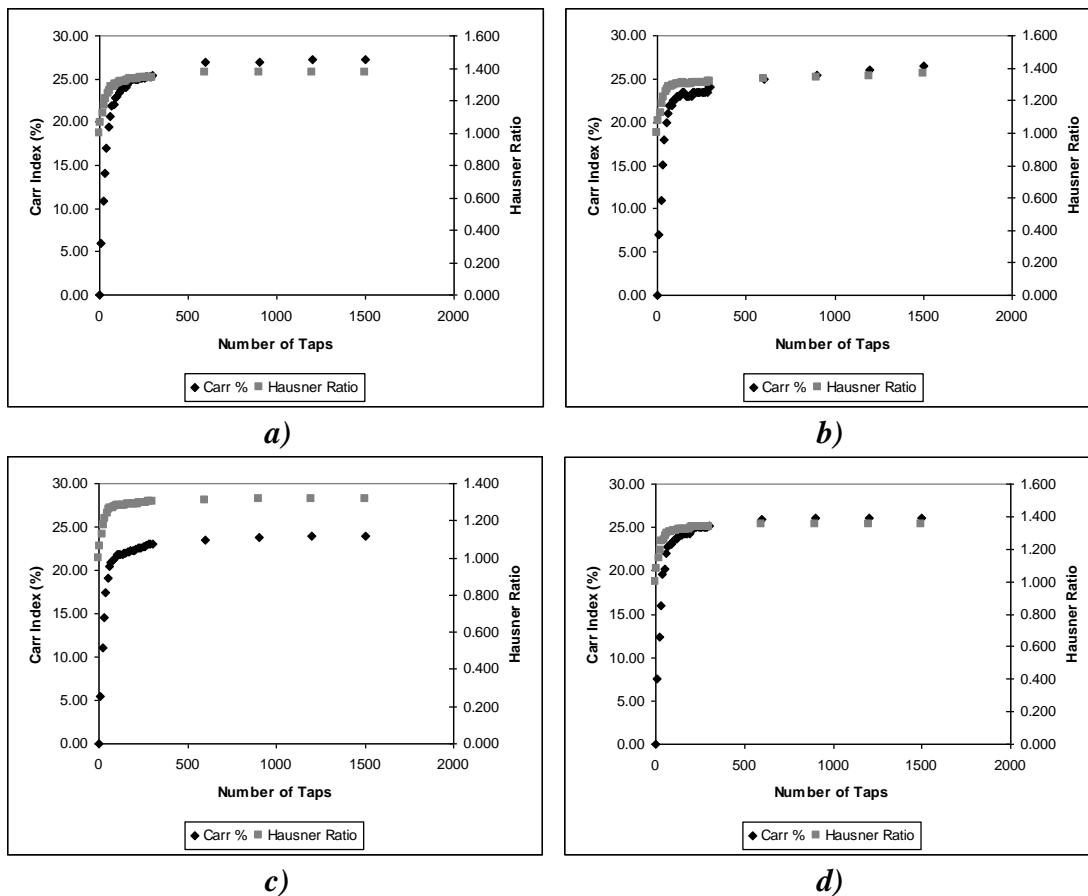


**Figure A.2: Compressibility of HPMC at (a) 0%, (b) 2%, (c) 5%, (d) 10% Moisture Content**

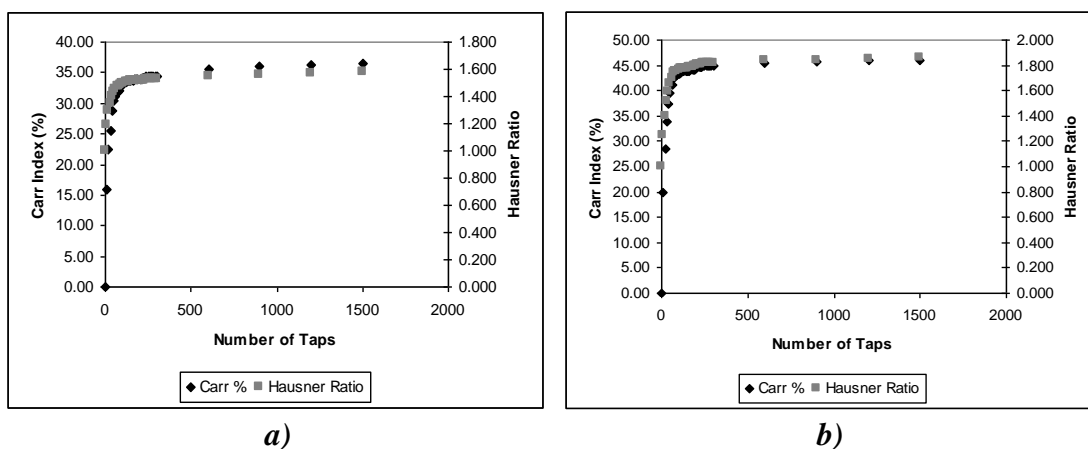


**Figure A.3: Compressibility of Nonhygroscopic Powders (a) API, (b) Respitose®**

## Appendix B: Static Angle of Repose Test Results

The following figures show results from the static angle of repose tests performed on the pharmaceutical powders. Only one test is shown for each powder moisture content.

Results from a total of three tests were averaged to obtain the values reported in Chapter 3.

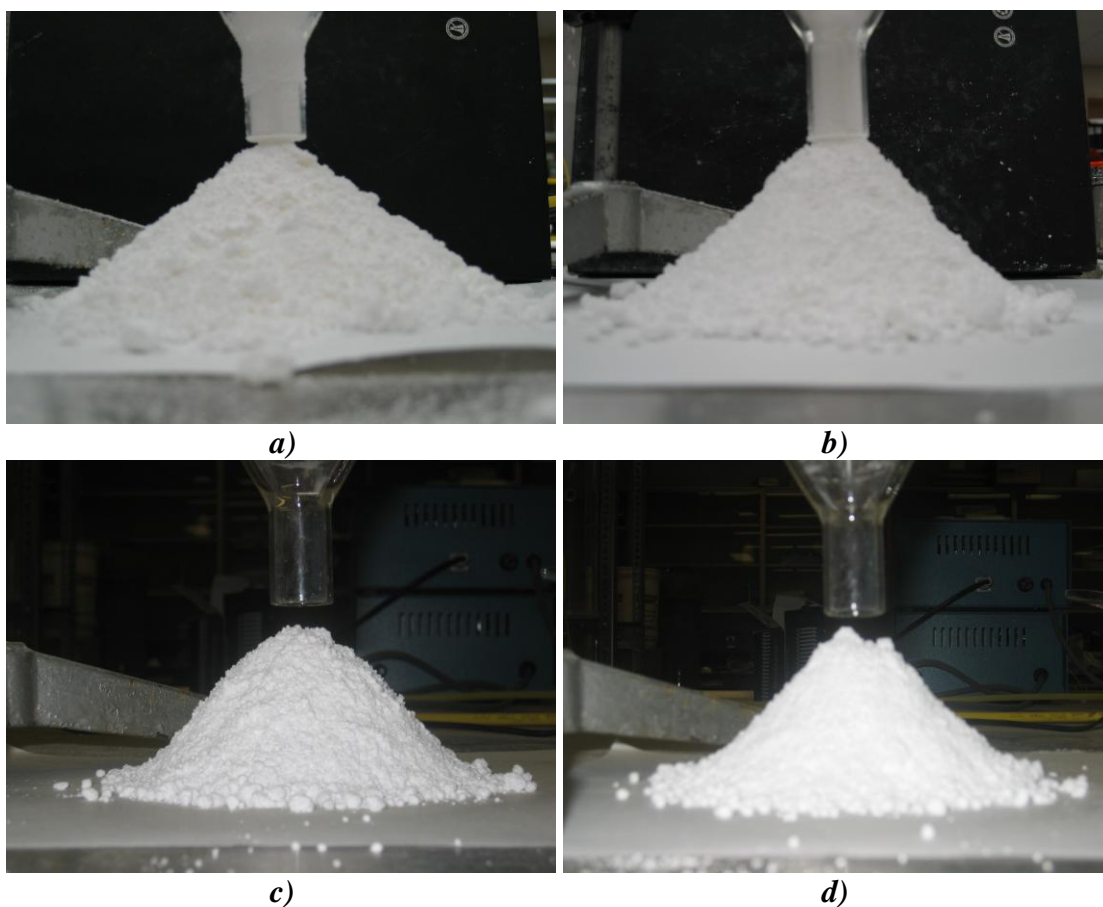


**Figure B.1: Static Angle of Repose of Aspartame at (a) 0%, (b) 2%, (c) 5%, (d) 8% Moisture Content**

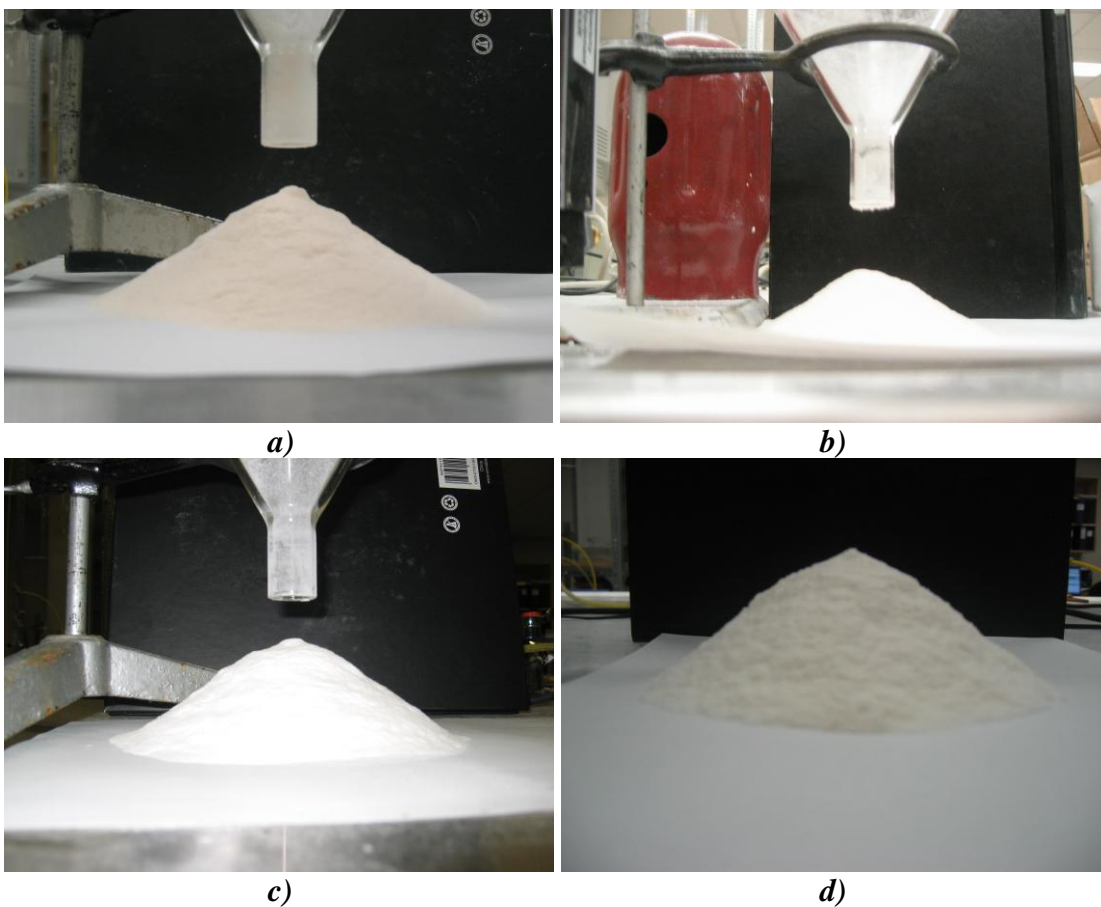


**Figure B.2: Static Angle of Repose of HPMC at (a) 0%, (b) 2%, (c) 5%, (d) 10% Moisture Content**

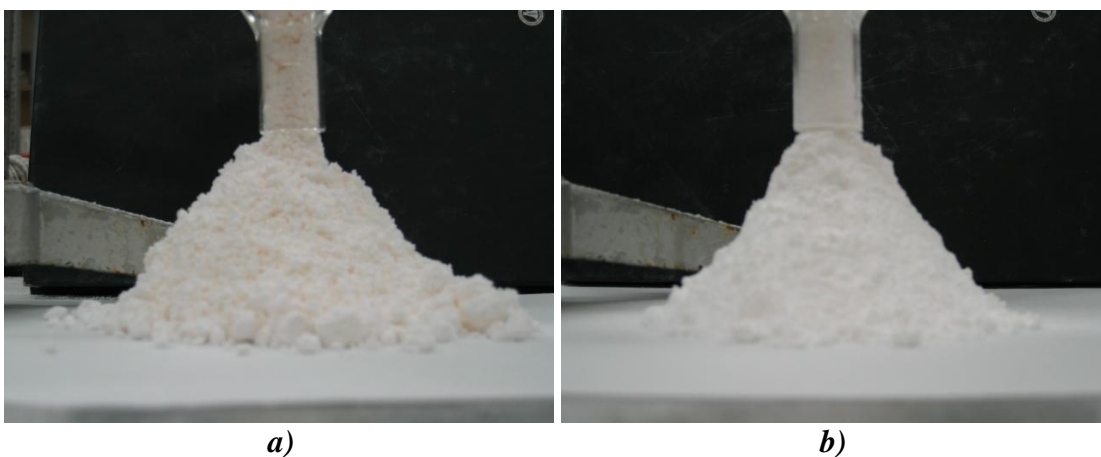


**Figure B.3: Static Angle of Repose of Nonhygroscopic Powders (a) API, (b) Respitose®**

## Appendix C: Dynamic Angle of Repose Test Results

The following figures show results from the dynamic angle of repose tests performed on the pharmaceutical powders. Only one image is shown for each test. The average of ten images taken during the last 10 seconds of the 100 second long test was reported as the dynamic angle of repose. This test was performed at each of 1 rpm, 3 rpm, and 7 rpm motor speeds. A total of two tests were averaged for each moist powder to obtain the values reported in Chapter 3.

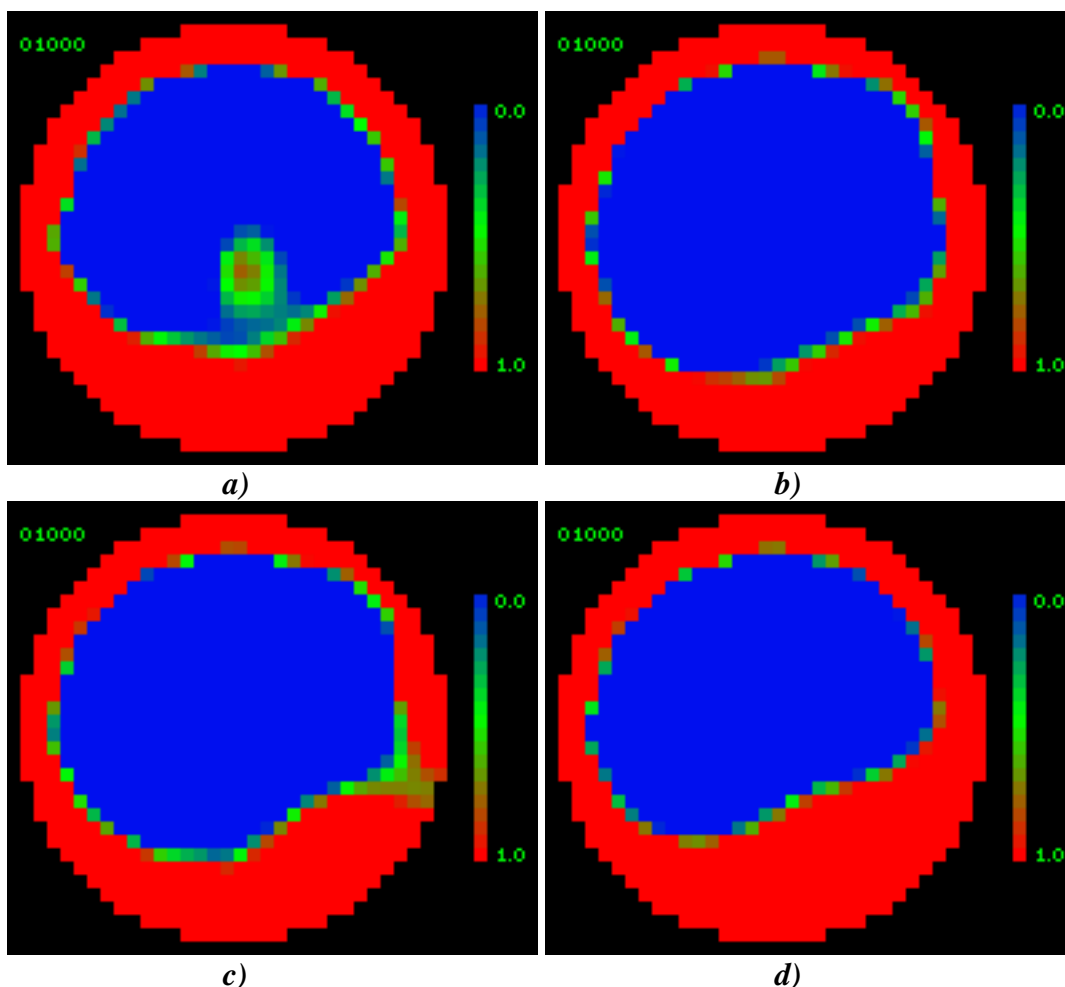


*Figure C.1: Dynamic Angle of Repose of Aspartame at (a) 0%, (b) 2%, (c) 5%, (d) 8% Moisture Content and 1 rpm*

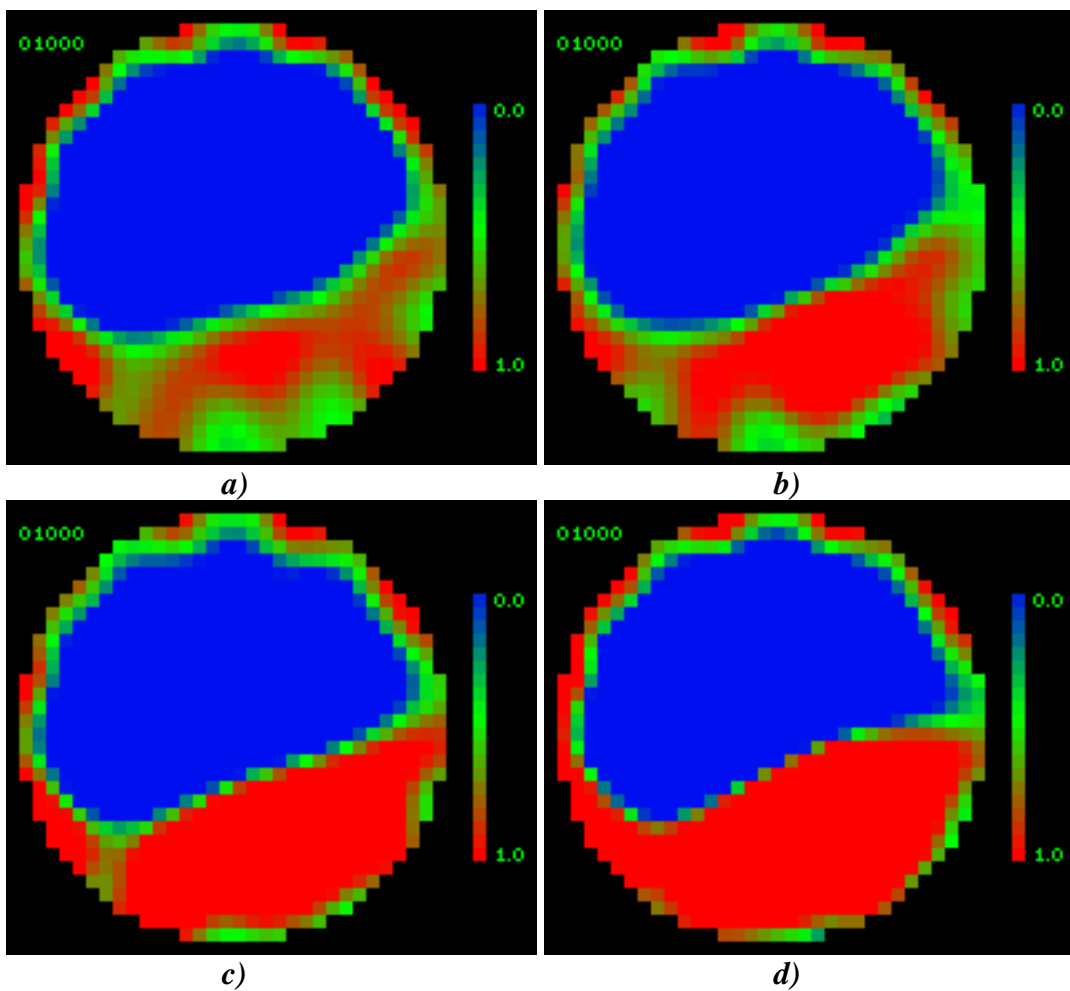


**Figure C.2: Dynamic Angle of Repose of HPMC at (a) 0%, (b) 2%, (c) 5%, (d) 10% Moisture Content and 1 rpm**

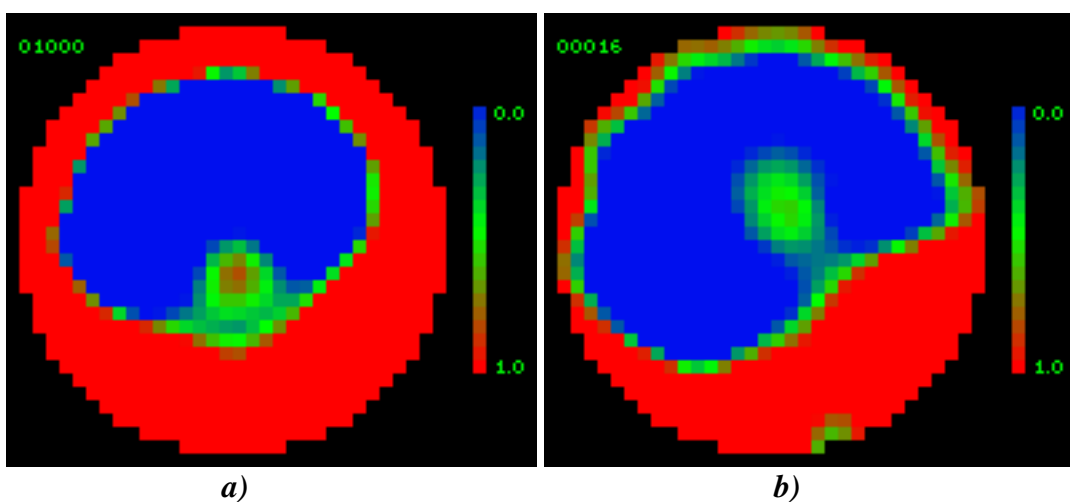


**Figure C.3: Dynamic Angle of Repose of Nonhygroscopic Powders (a) API, (b) Respitose® and 1 rpm**

## Appendix D: Jenike Shear Test Results

The following figures show results from the Jenike shear tests performed on the pharmaceutical powders. From a plot of shear stress at failure versus normal stress, the powder properties of cohesion (y-intercept), the angle of internal friction (slope), and the yield locus were calculated. From two Mohr's circles drawn tangent to the yield locus the unconfined yield strength and major consolidating stress at each pre-shear load could be determined. A plot of unconfined yield strength versus major consolidating stress is known as the Jenike flow function. The flow index,  $ff_c$ , is the inverse of the slope of the flow function, and represents the strength of a consolidated powder that must be overcome before flow can occur. A total of two tests were averaged for each powder to obtain the values reported in Chapters 3, 5, and 7.

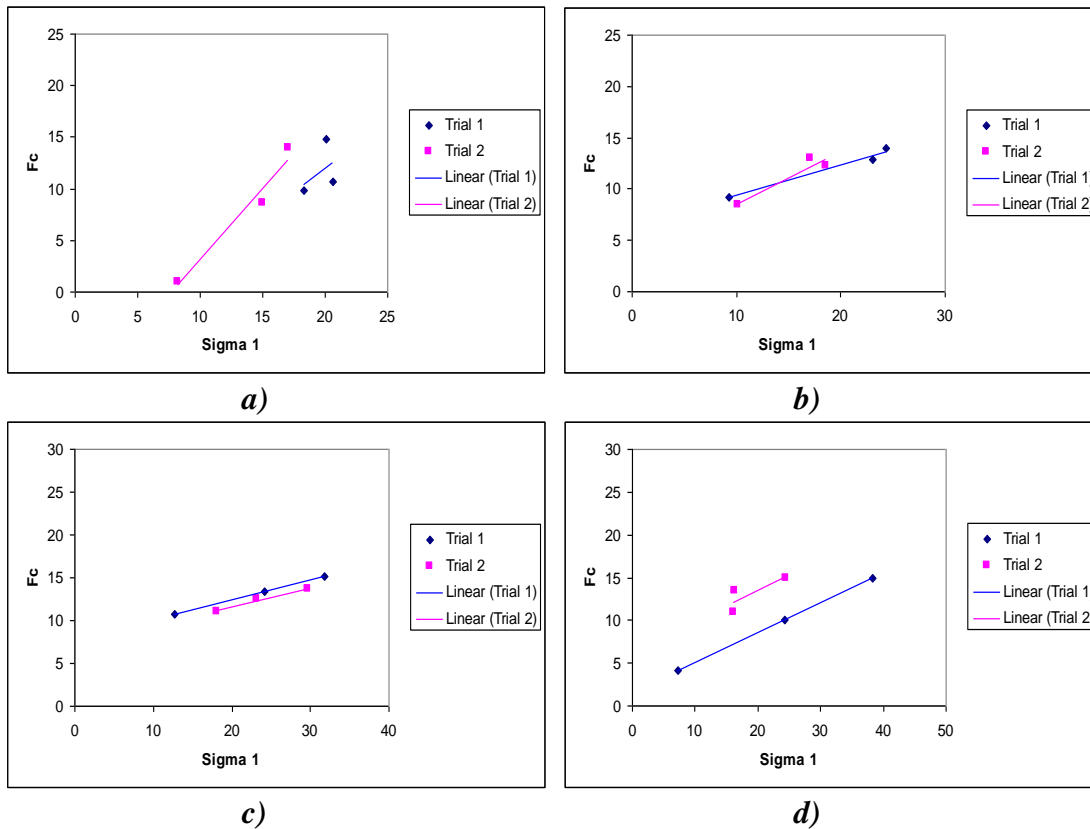


**Figure D.1: Jenike Flow Function of Aspartame at (a) 0%, (b) 2%, (c) 5%, (d) 8% Moisture Content**

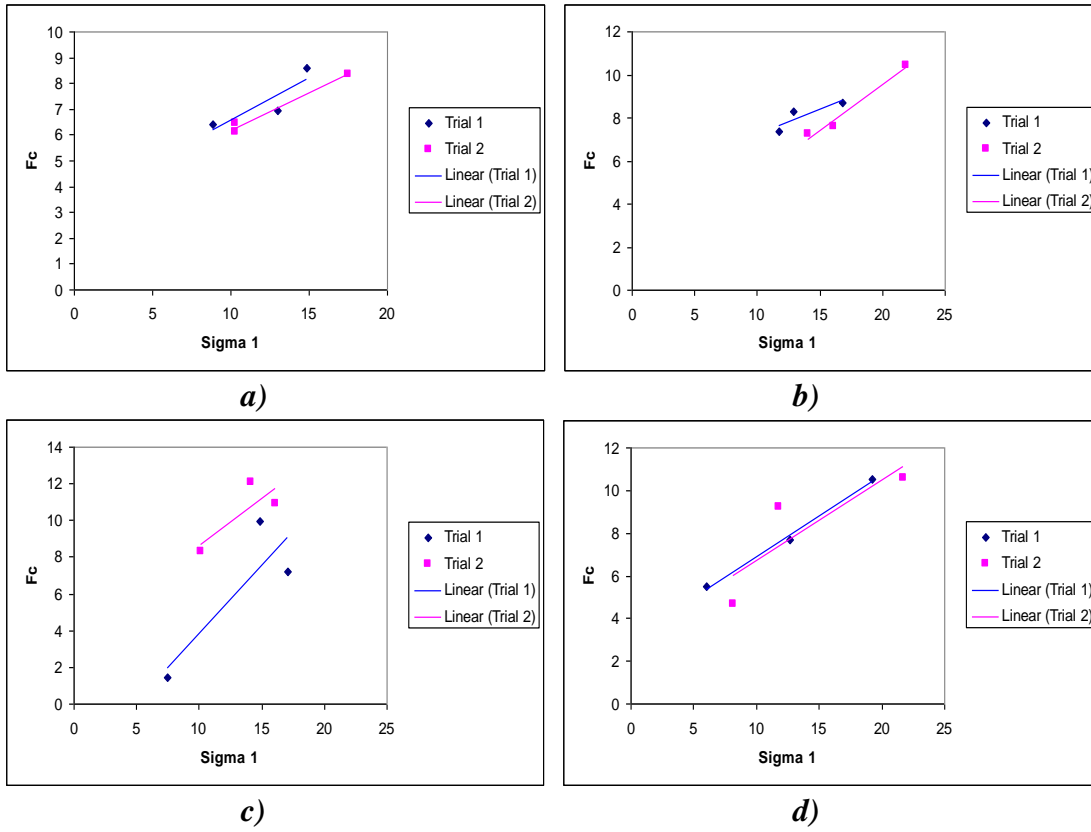


**Figure D.2: Jenike Flow Function of HPMC at (a) 0%, (b) 2%, (c) 5%, (d) 10% Moisture Content**

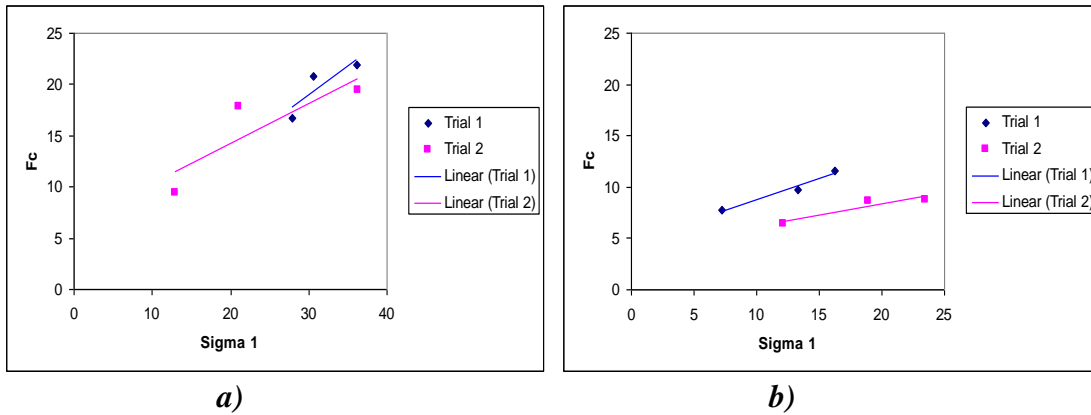
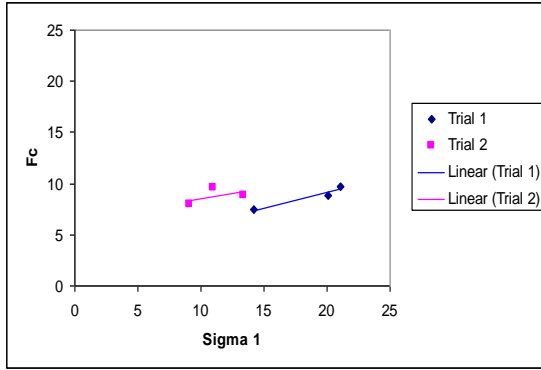
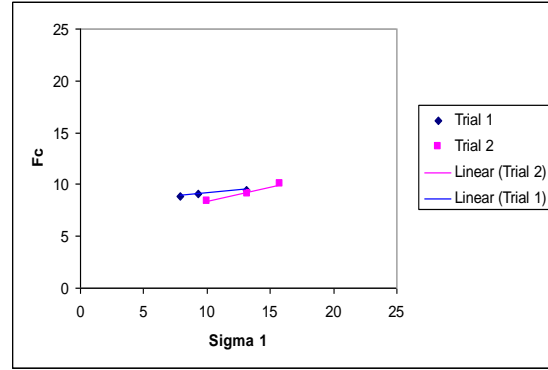


**Figure D.3: Jenike Flow Index of Nonhygroscopic Powders (a) API, (b) Respitose®**

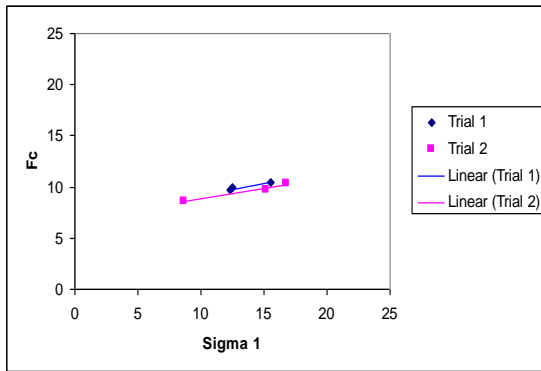




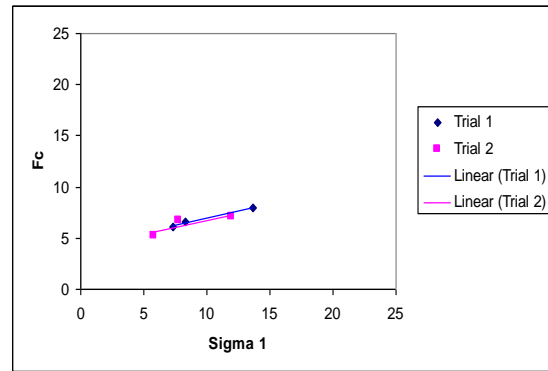
**a) Barley**



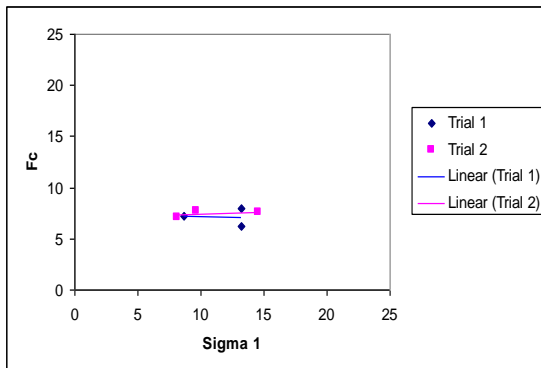
**b) Cow Cockle**



**c) Rice**

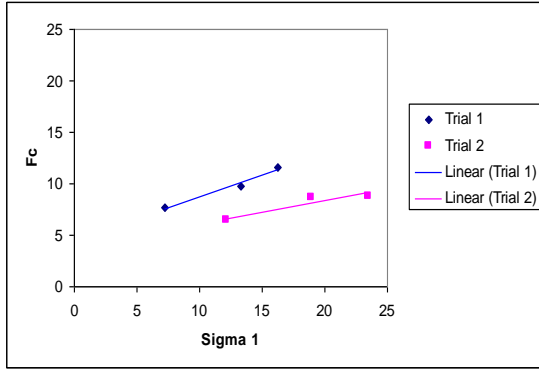


**d) Rye**

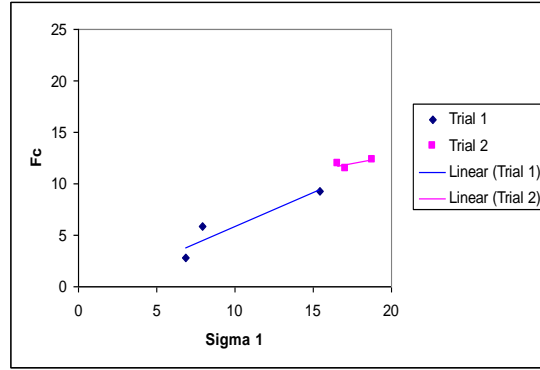


**e) Tapioca**

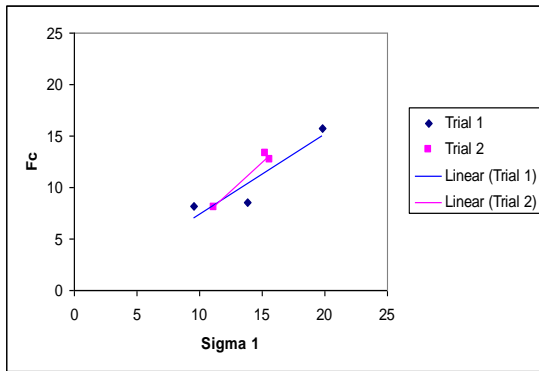
**Figure D.4: Jenike Flow Function of Starch Powders (a) Barley, (b) Cow Cockle, (c) Rice, (d) Rye, (e) Tapioca**



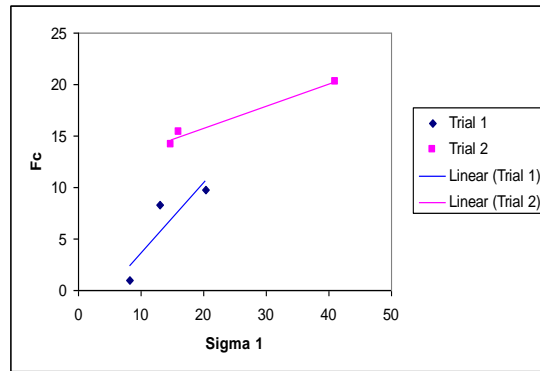
a)



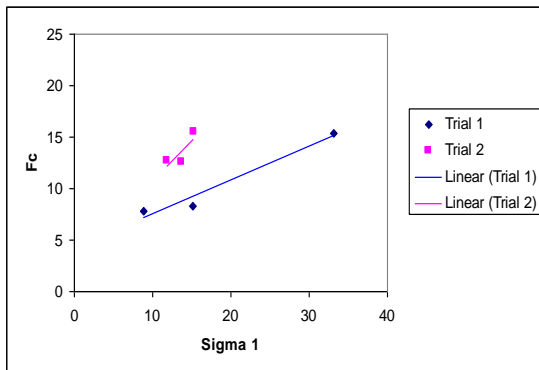
b)



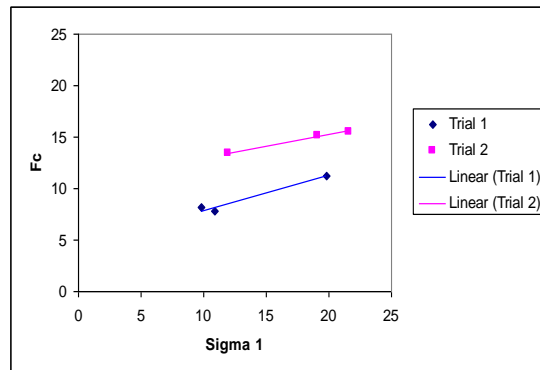
c)



d)



e)



f)

**Figure D.5: Jenike Flow Function of Ordered Mixtures (a) OM#1, (b) OM#2, (c) OM#3, (d) OM#4, (e) OM#5, (f) OM#6**

## Appendix E: Skeletal Density of Powders

Skeletal density (sometimes called “true density”) of the powders was measured using an Ultrapycometer (Ultrapycometer 1000, Quantachrome, Florida). It uses helium gas to fill the pore volume of the test powder, replacing all the air in the sample. A second chamber is then opened, allowing the pressure in the initial test chamber to drop. The density of the solid material in the test chamber is calculated from the pressure change resulting from this change in volume. The test is repeated between 3 and 15 times, until the standard deviation of the last three tests is less than 0.05g/cm<sup>3</sup>. The results for each of the powders investigated are given in Table E.1.

Table E.1: Skeletal Density

Powder	Skeletal Density (g/cc)
Barley	1.5019
Cow Cockle	1.5184
Rice	1.4997
Rye	1.4959
Tapioca	1.5036
API	1.2397
Aspartame	1.3827
HPMC	1.2838
Respitose®	1.5442